1   **The SUPECA kinetics for scaling redox reactions in networks of mixed substrates**

2   **and consumers and an example application to aerobic soil respiration**

3   Jinyun Tang and William J. Riley

4   Earth and Environmental Sciences Area, Lawrence Berkeley National Laboratory,

5   Berkeley, CA, USA, 94720

6   *Correspondence to*: J. Y. Tang (jinyuntang@lbl.gov)

7

8   **Abstract.** Several land biogeochemical models used for studying carbon-climate

9   feedbacks have begun explicitly representing microbial processes. However, to our

10   knowledge, there has been no theoretical work on how to achieve a consistent scaling of

11   the complex biogeochemical reactions from microbial individuals to populations,

12   communities, and interactions with plants and mineral soils. We here study this scaling

13   problem by focusing on the substrate-consumer relationships for consumer mediated

14   redox reactions of the form $A + B \xrightarrow{E} products$, where products could be microbial

15   biomass and different bio-products. Under the quasi-steady-state approximation, these

16   substrate-consumer relationships can be formulated as the computationally difficult full

17   Equilibrium Chemistry problem, which is then usually approximated analytically with the

18   popular Dual Monod (DM) kinetics and Synthesizing Unit (SU) kinetics. However, we

19   found that the DM kinetics is scaling inconsistent for reaction networks because it (1)

20   does not incorporate substrate limitation in its derivation, (2) invokes contradictory

21   assumptions regarding the substrate processing rate when transitioning from single

22   substrate reactions to two-substrate redox reactions, and (3) cannot scale the product

23   generation rate from one to multiple substrates. In contrast, the SU kinetics can

Geoscientific
Model Development
Discussions

1   consistently scale the product generation rate from one to multiple substrates, but suffers

2   from the deficit that as the consumer abundance approaches infinity, it predicts singular

3   infinite reaction rates even for limited substrates. We attribute this deficit to SU's failure

4   to incorporate the substrate limitation in its derivation and remedy SU with the proposed

5   SUPECA (SU Plus Equilibrium Chemistry Approximation) kinetics, which consistently

6   imposes the mass balance constraints from both substrates and consumers on consumer-

7   substrate interactions in calculating redox reaction rates. Moreover, we show the

8   SUPECA kinetics satisfies the partition principle as in theories like Newton's Law of

9   motion and Dalton's law of partial pressures, such that its mathematical manifestation is

10   scaling invariant when transitioning from an individual reaction to a network of many

11   reactions. We benchmarked the SUPECA kinetics with the equilibrium chemistry

12   solution for some simple problem configurations and found SUPECA outperformed the

13   SU kinetics. In applying the SUPECA kinetics to aerobic soil respiration, we found

14   SUPECA predicted consistent but variable moisture response functions that agreed well

15   to those derived from incubation data. We finally discuss how the SUPECA kinetics

16   could help Earth System Models consistently incorporate more biogeochemical reactions

17   to improve their biogeochemical modules.

18

19   **Keywords**: Dual-Monod kinetics, Synthesizing Unit, SUPECA kinetics, soil respiration,

20   trait-based modeling

21

22

23

Geoscientific
Model Development
Discussions

1. Introduction

Land holds more than twice the carbon that is in the atmosphere; therefore a small change in land carbon dynamics can imply significant feedbacks to the ongoing climate warming (Ciais et al., 2013). This has motivated intense research towards better understanding of Earth's land biogeochemical cycles, both for prediction and assessing the efficacy of climate mitigation and adaptation strategies. To date, however, soil biogeochemical models are suffering from high uncertainty (e.g., Arora et al., 2013; Bouskill et al. 2014; Friedlingstein et al., 2014; He et al. 2016). For instance, eight CMIP5 Earth System Models (ESMs) predicted that the net land carbon uptake varies from 22 to 456 PgC for the 2006-2100 period under the Representative Concentration Pathway 4.5 (RCP4.5; Shao et al., 2013). Similarly, the 16 CMIP5 ESM simulations analyzed in Todd-Brown et al. (2013) estimated the contemporary global soil carbon stocks ranging from 510 to 3040 PgC to 1 m depth, while the most recent empirical estimation is 1408±154 PgC to 1 m depth and 2060±217 Pg C to 2 m depth (Batjes, 2016). Therefore, it is urgent to improve our models' predictive power.

The predictive power of existing land biogeochemical models is plagued by uncertainties from structural design, numerical implementation, model parameterization, initial conditions, and forcing data (Tang and Zhuang, 2008; Tang et al., 2010; Luo et al., 2015; Wieder et al., 2015a; Blanke et al., 2016; Tang and Riley, 2016). Among them, developing better model structure and formulation has been identified as a priority. One proposed structural improvement is to include explicit microbial processes (Wieder et al., 2015b), which has recently been shown to enable better predictions of global soil carbon stocks (Wider et al., 2013), priming effects (Sulman et al., 2014), vertical soil carbon

1   profiles (Riley et al., 2014), and respiratory temperature sensitivity (Tang and Riley,

2   2015). A second major proposal is to explicitly resolve the ecosystem nutrient cycle,

3   which aligns with the hypothesis that the potential for increasing land ecosystem carbon

4   uptake resulting from the effect of atmospheric CO_2 fertilization could be limited by

5   nutrient availability (Vitousek, 1982; Shi et al., 2015; Wieder et al., 2015c).

6   A common process that underlies both of these two proposed structural

7   improvements is the substrate-consumer interaction, which is fundamental for modeling

8   microbial decomposition of substrates (Tang and Riley, 2013a; Riley et al., 2014; Le

9   Roux et al., 2016), mineral soil interaction with adsorptive substrates (Tang and Riley,

10   2015), and plant-microbe competition for nutrients (Zhu et al., 2016a, 2016b, 2016c). In

11   soil, because there are many consumers competing for many substrates in different places

12   at different times, the biogeochemical models being developed must be able to scale the

13   many biogeochemical processes consistently across space, time, and processes. Of the

14   three dimensions that call for scaling (Figure 1), scaling across the spatial and temporal

15   dimensions is achieved through spatial and temporal discretization and integration, which

16   has been intensively studied elsewhere (e.g., Kolditz et al., 1998; Mao et al., 2006), so

17   here we study the scaling along the less studied third dimension—process—with a focus

18   on substrate-consumer interactions.

19   Within a certain homogeneous space-time-process unit in soil (Figure 1), there are

20   generally three types of substrate-consumer relationships: (1) single-substrate Monod

21   type reactions in the form of $A \xrightarrow{E} products$; (2) the two-substrate redox reactions in the

22   form of $A + B \xrightarrow{E} products$, where substrate A and B are called complementary because

4

Geoscientific
Model Development
Discussions

1   they both are required to proceed the redox reaction; and (3) the multi-substrate (>2)

2   reactions $\sum_i A_i \xrightarrow{E} products$. The scaling of the single-substrate Monod type reaction has

3   been extensively discussed in Tang and Riley (2013a), and is resolved with the

4   Equilibrium Chemistry Approximation (ECA) kinetics (and more discussion on the ECA

5   kinetics for process scaling will be provided in later sections when discussing the

6   SUPECA kinetics). Further, because many multi-substrate reactions can be separated into

7   a combination of single-substrate reactions and redox-reactions, it is important to achieve

8   consistent kinetic scaling from a single redox reaction to many reactions in a network.

9   Mathematically, the problem should be addressed with explicit formulation of all

10   kinetic processes using ordinary differential equations accounting for all substrates and

11   consumers (Chellaboina et al., 2009). However, such a formulation would require too

12   many parameters to drive the model and is numerically very difficult to solve because of

13   its multi-temporal scale nature. By making the quasi-steady-state-approximation (QSSA),

14   i.e., assuming that the product generation from consumer-substrate complex is much

15   slower than the equilibration between consumers, substrates, and consumer-substrate

16   complexes (Briggs and Haldane, 1925), the full kinetic problem is reduced to the simpler

17   Equilibrium Chemistry (EC) form (e.g., Chellaboina et al., 2009). However, the EC form

18   is also usually very difficult to solve numerically. Therefore, analytical approximations to

19   the EC formulation are generally made.

20   Two classic analytical approximations for modeling redox-reactions are the Dual

21   Monod (DM) kinetics (e.g., Yeh et al., 2001) and Synthesizing Unit (SU) approach

22   (Kooijman, 1998; Brandt et al., 2003). Although both of them are a special case of the EC

23   formulation (Kooijman, 2010; Tang and Riley, 2013a), they make different assumptions

1   of the relative magnitudes of the involved kinetic parameters. For this, Kooijman (2010)

2   has shown that the DM kinetics inevitably requires the dissociate rate to be much larger

3   than the product-generation rate from the consumer-substrate complexes. In contrast, to

4   apply the single-substrate Monod kinetics (Monod, 1949) or Michaelis-Menten (MM)

5   kinetics (Michaelis and Menten, 1913; which is mathematically identical to the empirical

6   Monod kinetics and they two will be used interchangeably hereafter) does not impose this

7   requirement on its parameters. Moreover, in applications to r-K scaling (e.g., Litchman

8   and Klausmeier, 2008), the single-substrate Monod kinetics even requires the product-

9   generation rate to be faster than the dissociation rate of the consumer-substrate

10 complexes. This contrasting requirement on parameters, as we will show later, fails the

11 DM kinetics to achieve a consistent scaling of substrate-consumer interactions for generic

12 biogeochemical modeling.

13   We define a kinetic formulation to have consistent scaling when the formulated

14 substrate-consumer relationship: (1) can seamlessly transition from a single substrate-

15 consumer pair to a network of many substrate-consumer pairs without changing its

16 mathematical forms (aka the partition principle) and (2) does not predict any singularity

17 over the whole range of substrate and consumer concentrations (aka the non-singular

18 principle). The full kinetics formulation and its EC formulation both satisfy these two

19 criteria, which can be explained using the following example network of consumer-

20 substrate relationships:

$$S_i + E_j \underset{k_{1,ij}^-}{\overset{k_{1,ij}^+}{\longleftrightarrow}} E_j S_i \overset{k_{2,ij}^+}{\longrightarrow} P_{ij} + E_j \tag{1}$$

Geoscientific
Model Development
Discussions

1   where substrate S_i complexes with consumer E_j to form complex $E_j S_i$, which is then

2   degraded into product P_{ij} and the free consumer. In equation (1) (and throughout this

3   study), the forward kinetic parameters are indicated with superscript "+", while the

4   backward kinetic parameters are with superscript "−". Here and below we assume that the

5   units of all variables are consistently defined, and they are only put forward explicitly

6   when it is necessary to resolve an ambiguity.

7   The full kinetic formulation for the network of equation (1) is:

$$\frac{d[S_i]}{dt} = -[S_i]\sum_j\left(k_{1,ij}^+[E_j]\right) + \sum_j\left(k_{1,ij}^-[E_j S_i]\right) \tag{2}$$

$$\frac{d[E_j S_i]}{dt} = k_{1,ij}^+[S_i][E_j] - \left(k_{1,ij}^- + k_{2,ij}^+\right)[E_j S_i] \tag{3}$$

$$\frac{d[E_j]}{dt} = -[E_j]\sum_i\left(k_{1,ij}^+[S_i]\right) + \sum_i\left(\left(k_{1,ij}^- + k_{2,ij}^+\right)[E_j S_i]\right) \tag{4}$$

8   where, and also throughout this study, we use $[x]$ to indicate the concentration of x.

9   That the full kinetic formulation is consistent with the partition principle is

10   manifested in the first summation in equations (2) and (4). Particularly for equation (4),

11   by defining an appropriate mean specific substrate affinity $k_{1,j}^+$, the summation

12   $\sum_i\left(k_{1,ij}^+[S_i]\right)$ can be recast into the form $\sum_i k_{1,ij}^+[S_i] = k_{1,j}^+[S]$, in which $[S] = \sum_i[S_i]$

13   resembles Dalton's law of partial pressures (and many other similar relationships in

14   physics, e.g., Newton's second law of motion (Feynman et al., 1963)) and is clearly

15   partition consistent.

1   Meanwhile, that the full kinetic formulation satisfies the nonsingular principle can

2   be verified by noting that, at any time:

$$\left[S_i\right] + \sum_j \left[E_j S_i\right] = \left[S_i\right]_T \tag{5}$$

3   and that the consumption of S_i is through the generation of product from $\left[E_j S_i\right]$.

4   Therefore, by combining equations (2), (3), and (5), the overall consumption rate of S_i

5   (i.e., $\sum_j k_{2,ij}^+\left[E_j S_i\right]$) is always smaller than $\left[S_i\right]_T \sum_j k_{2,ij}^+$.

6   Since the EC formulation is obtained by applying QSSA to the full kinetic

7   formulation (i.e., $d\left[E_j S_i\right]\big/dt \approx 0$ for equation (3)), it automatically satisfies the two

8   criteria for consistent process scaling. However, the Monod kinetics is scaling

9   inconsistent when it is applied, for example, to the single-substrate competition by

10   multiple populations, or to the multi-substrate consumption by a single population. (e.g.,

11   Williams, 1973; Allison, 2012; Tang et al., 2010; Riley et al., 2011, 2014; Bouskill et al.,

12   2012; Wieder et al., 2013, 2014). Specifically, the Monod kinetics violates the partition

13   principle, which can be shown from the following inequality:

$$F_j = \left[E_j\right]\sum_i \frac{k_{2,ij}^+\left[S_i\right]}{K_{ij}+\left[S_i\right]} \neq \left[E_j\right]\frac{\sum_i k_{2,ij}^+\left[S_i\right]\big/K_{ij}}{1+\sum_i \left[S_i\right]\big/K_{ij}} \tag{6}$$

14   Here F_j describes the uptake of all substrates S_i by population E_j. The left hand side of

15   the inequality is the uptake computed by directly applying the Monod kinetics, while the

16   right hand side of the inequality is by applying the competitive Monod kinetics

17   (Litchman and Klausmeier, 2008). The inequality (6) is even true when K_{ij} is independent

Geoscientific
Model Development
Discussions

1   of i. Besides being inconsistent with the partitioning principle, the Monod kinetics also

2   violates the non-singular principle, which can be demonstrated by observing that, as

3   $\left[E_j\right]$ approaches infinity, so does F_j.

4   For the competitive Monod kinetics on the right hand side of the inequality in

5   equation (6) (e.g., Murdoch, 1973), if all substrates have the same affinity parameter (i.e.,

6   $K_j = K_{ij}$), we have the following

$$F_j = \left[E_j\right] \frac{k_{2,j}^+ \left(\sum_i \left[S_i\right]\right)\Big/ K_j}{1 + \left(\sum_i \left[S_i\right]\right)\Big/ K_j} = \left[E_j\right] \frac{k_{2,j}^+ \left[S\right]\Big/ K_j}{1 + \left[S\right]\Big/ K_j} \tag{7}$$

7   where $\left[S\right] = \sum_i \left[S_i\right]$ designates the total free concentrations of all substrates. Equation

8   (7) therefore suggests that the competitive Monod kinetics satisfies the partition principle

9   for consistent scaling of substrate-consumer relationships. Nevertheless, because the

10 competitive Monod kinetics is linear in $\left[E_j\right]$, like the classic Monod kinetics, it still

11 violates the non-singular principle for consistent scaling.

12   In Tang (2015), it was shown that the linear dependence of F_j on $\left[E_j\right]$ as

13 predicted by the Monod kinetics and similarly by the competitive Monod kinetics is due

14 to their failure to impose the substrate mass (or surface area) balance in deriving their

15 mathematical formulations. This problem has been rectified in the Equilibrium Chemistry

16 Approximation kinetics (Tang and Riley, 2013a), which was shown to predict much more

17 accurate parametric sensitivity than the Monod kinetics in comparing with analytical

18 solutions (Tang, 2015). Since the success of all model calibrations rely on the sensitivity

1   of model predicted responses with respect to model parameters (e.g., Wang et al., 2001;

2   Williams et al, 2005; Tang and Zhuang, 2009), ensuring that the substrate kinetics

3   predicts accurate parametric sensitivity is essential for developing robust biogeochemical

4   models.

5   We therefore ask the question: how should we achieve a consistent scaling from

6   the simplest redox reaction $A + B \xrightarrow{E} products$ (i.e., AB-E type) to a network that mixes

7   many redox reactions and even single substrate Monod-type reactions (a situation found

8   commonly in nature)? Aside from the two criteria (i.e., the partition principle and non-

9   singularity) discussed above, we suggest a third criterion that a consistent scaling of

10   substrate-consumer relationships should be able to seamlessly transition from a single

11   substrate Monod-type reaction to the AB-E type redox reaction without making

12   contradictory assumptions in its theoretical derivation.

13   In the following, we address the above question by first presenting the step-by-

14   step derivation of the DM kinetics and the SU kinetics from the EC formulation of the

15   redox reaction $A + B \xrightarrow{E} products$. Conceptually, DM kinetics can be viewed as a straight

16   application of chemical kinetics that the reaction rate of substrates A and B over

17   consumer E is determined by the product of A and B's binding probability to E (which in

18   Monod form is $\left[A \right] / \left(K_A + \left[A \right] \right)$ for substrate A, and $\left[B \right] / \left(K_B + \left[B \right] \right)$ for substrate B).

19   Kooijman (1998) was the first to derive the SU kinetics using the queue theory (e.g.,

20   Gross et al., 2011) and Brandt et al. (2003) discussed its use for AB-E type redox

21   reactions. The following derivation will stress on exposing the scaling-inconsistencies

22   implied in the DM kinetics and SU kinetics, and, in particular, we will show that DM
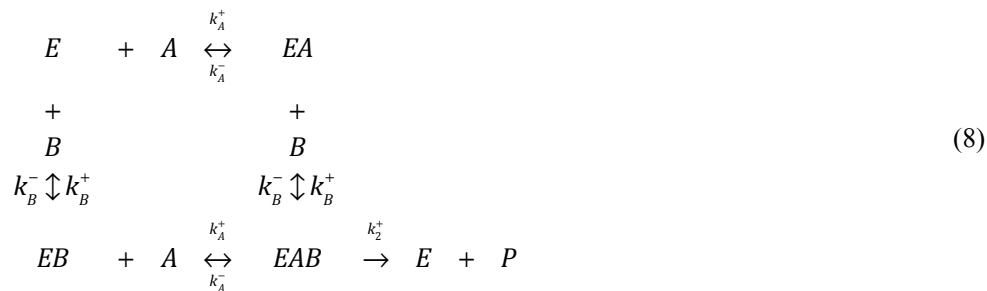
1   kinetics cannot be extended for consistent process scaling. We then present the SUPECA

2   kinetics that remedies the inconsistencies of the SU kinetics. We demonstrate the benefits

3   of SUPECA in terms of its numerical accuracy and present an example application of

4   modeling the moisture control of aerobic soil respiration. Finally, we discuss how one

5   can apply the SUPECA kinetics to trait-based modeling approaches in various

6   biogeochemical systems.

7   **2. Derivation of ECA kinetics for AB-E type redox reaction** $A+B\xrightarrow{E}products$

8   **2.1 Governing equations**

9   We schematically represent the enzymatic redox reaction network as

$$
\begin{array}{ccccc}
E & + & A & \underset{k_A^-}{\overset{k_A^+}{\leftrightarrow}} & EA \\
+ & & & & + \\
B & & & & B \\
k_B^- \updownarrow k_B^+ & & & & k_B^- \updownarrow k_B^+ \\
EB & + & A & \underset{k_A^-}{\overset{k_A^+}{\leftrightarrow}} & EAB \xrightarrow{k_2^+} E + P
\end{array}
\tag{8}
$$

10   where it is assumed that the order of substrates A and B's binding to consumer E does not

11   affect the kinetic coefficients as is done in most modeling studies (e.g., Yeh et al., 2001).

12   By law of mass action and the total QSSA (tQSSA; e.g., see Borghans et al.,

13   1996; Tang and Riley, 2013a), we have the governing equations (see appendix A for

14   derivations) as follows:

$$
\frac{d\left[A\right]_T}{dt}=-k_2^+\left[EAB\right]
\tag{9}
$$

$$
\frac{d\left[B\right]_T}{dt}=-k_2^+\left[EAB\right]
\tag{10}
$$

$$k_A^+[E][A] + k_B^-[EAB] = \left(k_A^- + k_B^+[B]\right)[EA] \tag{11}$$

$$k_B^+[E][B] + k_A^-[EAB] = \left(k_B^- + k_A^+[A]\right)[EB] \tag{12}$$

$$k_A^+[EB][A] + k_B^+[EA][B] = \left(k_A^- + k_B^- + k_2^+\right)[EAB] \tag{13}$$

1   where

$$[A]_T = [A] + [EA] + [EAB] \tag{14}$$

$$[B]_T = [B] + [EB] + [EAB] \tag{15}$$

$$[E]_T = [E] + [EA] + [EB] + [EAB] \tag{16}$$

2   The derivation of substrate kinetics is therefore equivalent to solving for $[EAB]$ from the

3   EC problem defined by equations (11)-(16). However, because this set of equations is

4   non-linear, and no analytical solutions are available (to our knowledge), some

5   linearization is warranted to obtain analytical approximations. And as we describe below,

6   linearization with different assumptions lead respectively to the DM, SU, and SUPECA

7   kinetics.

8   2.2 **Dual Monod kinetics and synthesizing unit kinetics**

9   One method to linearize equations (11)-(16) is to assume that the concentration of

10   consumer-substrate complexes are so small that the free substrate concentrations are

11   equal to the bulk concentrations (e.g., for substrate A, it holds $[A]_T = [A]$). This

12   approach when combined with different assumptions on the relative magnitudes of the

13   kinetic parameters then leads to the popular DM kinetics and the two-substrate SU

14   kinetics.

1 **2.2.1 Dual Monod kinetics**

2 We now derive the DM kinetics. Adopting the equilibrium approximation that the

3 forward binding between consumer and substrate is in rapid equilibrium with the

4 backward dissociation of the consumer-substrate complex (e.g., Michaelis and Menten,

5 1913; Pyun, 1971), we have the following

$$\left[EA\right]\left[B\right]=\frac{k_B^-}{k_B^+}\left[EAB\right]=K_B\left[EAB\right] \tag{17}$$

$$\left[EB\right]\left[A\right]=\frac{k_A^-}{k_A^+}\left[EAB\right]=K_A\left[EAB\right] \tag{18}$$

6 which then transforms equations (11) and (12) into

$$\left[E\right]\left[A\right]=\frac{k_A^-}{k_A^+}\left[EA\right]=K_A\left[EA\right] \tag{19}$$

$$\left[E\right]\left[B\right]=\frac{k_B^-}{k_B^+}\left[EB\right]=K_B\left[EB\right] \tag{20}$$

7 By solving $\left[EAB\right]$ from equations (14)-(16) using equations (17)-(20), we obtain

8 the consumer-substrate complex for the DM kinetics (see Appendix B)

$$\frac{d\left[A\right]_T}{dt}=-k_2^+\left[E\right]_T\frac{\left[A\right]}{K_A+\left[A\right]}\frac{\left[B\right]}{K_B+\left[B\right]} \tag{21}$$

9 Although as one substrate, e.g., $\left[A\right]$, approaches infinity, equations (21) can be

10 reduced to the classical MM kinetics

$$\frac{d\left[A\right]_T}{dt}=-k_2^+\frac{\left[E\right]_T\left[B\right]}{K_B+\left[B\right]} \tag{22}$$

1   we note that the half saturation coefficient $K_B = k_B^- / k_B^+$ in equation (22) is different from

2   its usual definition, which should be $K_B = \left(k_2^+ + k_B^- \right) / k_B^+$, if one derives the MM kinetics

3   rigorously starting from a single substrate and single consumer system (e.g., Tang, 2015).

4   For this reason, we assert that the DM kinetics cannot achieve a self-consistent scaling

5   from one-substrate reaction to multiple-substrate reactions. More specifically, by

6   substituting equations (17) and (18) into equation (13), one obtains $k_2^+ = 0$, or at least

7    $k_2^+ \ll \max\left(k_A^-, k_B^- \right)$, which states that the consumer is very inefficient in processing the

8   substrate. However, MM kinetics does not require the dissociation rate to be much higher

9   than the product generation rate from the consumer-substrate complex, i.e.

10    $k_2^+ \ll \max\left(k_A^-, k_B^- \right)$ (e.g., Briggs and Haldane, 1925). Nor do the high dissociation rates of

11    $\left[EA \right]$, $\left[EB \right]$, and $\left[EAB \right]$ favor the consumer's assimilation of substrates under usual

12   substrate concentrations (e.g., Van Slyke and Cullen, 1914), even though a high

13   dissociation rate may possess some theoretical advantage under high substrate

14   concentrations when the consumer is a single enzyme (Reuveni et al., 2014). To the

15   contrary, most existing applications tend to assume $k_2^+ \gg k_A^-$ and $k_2^+ \gg k_B^-$ (e.g., Holling,

16   1959, 1966; Aksnes and Egge, 1991; Armstrong, 2008; Bonachela et al., 2011), such that

17    $K_B \approx k_2^+ / k_B^+$ for MM kinetics and the r-K selection can be explained (by linking k_2^+ with

18   growth rate, and k_A^+ and k_B^+ with substrate competitive ability; e.g., Litchman and

19   Klausmeier, 2008). Therefore, for biogeochemical modeling, DM and MM (or Monod)

Geoscientific
Model Development
Discussions

1   kinetics are based on different assumptions of the kinetic parameters, and the smooth

2   transition from DM to single substrate Monod kinetics is only ostensible.

3   **2.2.2 Synthesizing unit kinetics**

4   In deriving the SU kinetics for the redox reaction network represented in equation

5   (8), consumer E is viewed as a generalized enzyme that generates bio-products by

6   processing substrates A and B. SU computes the specific reaction rate per unit

7   concentration of E as the product generation rate k_2^+ times the probability that E binds

8   together with both substrates A and B (which is $[EAB]/[E]_T$). Mathematically, SU

9   kinetics requires the sufficient flux condition $k_A^+[A] \gg k_B^-$ and $k_B^+[B] \gg k_A^-$ (Kooijman,

10 2010). Define $\tilde{k}_2^+ = k_A^- + k_B^- + k_2^+$, equations (11)-(13) become

$$k_A^+[E][A] = k_B^+[B][EA] \tag{23}$$

$$k_B^+[E][B] = k_A^+[A][EB] \tag{24}$$

$$k_A^+[EB][A] + k_B^+[EA][B] = \tilde{k}_2^+[EAB] \tag{25}$$

11 From equations (23)-(25), we obtain (see Appendix C)

$$\frac{d[A]_T}{dt} = -\frac{k_2^+[E]_T / \tilde{k}_2^+}{\dfrac{1}{\tilde{k}_2^+} + \dfrac{1}{k_A^+[A]} + \dfrac{1}{k_A^+[B]} - \dfrac{1}{k_A^+[A] + k_A^+[B]}} \tag{26}$$

12   The two-substrate SU kinetics as indicated by equation (26) can be viewed

13 alternatively as a special case of the general SU kinetics for any number of

14 complementary substrates, which was derived by Kooijman (1998) based on the queue

15 theory (e.g., Gross et al., 2011). Kooijman (1998) assumed that the consumers act like

1   synthesizing units, which process the substrates in two steps: binding and production. He

2   then assumed that all flux rates (including production rates k_2^+ and substrate binding

3   rates $k_A^+[A]$ and $k_B^+[B]$) are of Poisson distributions, and calculated the overall specific

4   substrate consumption rate as the reciprocal of the expected total processing time (i.e., the

5   denominator of equation (26)). The last term in the denominator of equation (26) comes

6   from the assumption of parallel binding of substrates A and B to E, and it disappears if

7   sequential binding is assumed.

8   As one substrate, e.g., A, approaches infinity, the single-substrate Monod kinetics

9   is recovered from equation (26):

$$\frac{d[A]_T}{dt} = -\frac{k_2^+[E]_T}{1+\dfrac{\tilde{k}_2^+}{k_B^+[B]}} = -\frac{k_2^+[E]_T[B]}{\dfrac{\tilde{k}_2^+}{k_B^+}+[B]} \tag{27}$$

10   which has a half saturation coefficient similar to what would be derived for a single

11   substrate, single consumer reaction (e.g., Tang, 2015). By assuming Poisson distribution

12   of the kinetic parameters, it can also be shown for a single enzyme molecule that MM

13   kinetics represents the statistical mean of the fluctuating activity of the enzyme (English

14   et al., 2006; Reuveni et al., 2014). That the kinetics of both single-substrate reaction and

15   two-substrate redox reaction can be similarly derived using statistical theory and that

16   equations (26) and (27) could be obtained from EC formulation using consistent

17   assumptions of the kinetic parameters indicate, in contrast to DM kinetics, that SU

18   kinetics is able to scale consistently between one-substrate and two-substrate redox

19   reactions.

Geoscientific
Model Development
Discussions

1 **2.3. SUPECA kinetics**

2   In Tang (2015), it was shown that the derivation of MM kinetics ignores the mass

3 balance constraint of substrate, resulting in the MM kinetics to predict inaccurate

4 parametric sensitivity over the wide range of substrate to consumer ratios (e.g., Figure 1

5 in Tang (2015)). In the above, we also noticed that the substrates mass balance

6 constraints as indicated by equations (14) and (15) are not used in deriving the DM and

7 SU kinetics, suggesting that both the DM and SU kinetics may suffer from the same

8 deficit as the MM kinetics. Further, since the DM kinetics fails to consistently scale from

9 a single substrate to two complementary substrates, we below only remedy the SU

10 kinetics into the SUPECA kinetics to achieve a scalable and non-singular formulation of

11 the redox reactions.

12   As implied in equations (9)-(16), the derivation of substrate kinetics requires

13 solving for $\left[EAB \right]$ from nonlinear equations (11)-(16), whose analytical solutions are not

14 available. To obtain improved solutions as compared to SU kinetics, we applied a first

15 order closure approach (appendix D) to the system formed by equations (11)-(16),

16 leading to the SUPECA kinetics:

$$
\begin{aligned}
\frac{d[A]_T}{dt} &= -\frac{[E]_T}{\dfrac{1}{k_2^+}\dfrac{\overline{f}_A\overline{f}_B f_{AB}}{f_A f_B \overline{f}_{AB}} + \dfrac{1}{f_A} + \dfrac{1}{f_B} - \dfrac{f_A\overline{f}_B + \overline{f}_A f_B - \overline{f}_A\overline{f}_B}{f_A f_B \overline{f}_{AB}}} \\
&= -\frac{k_2^+[E]_T\left(f_A/k_2^+\right)\left(f_B/k_2^+\right)}{\dfrac{\overline{f}_A\overline{f}_B}{k_2^+\overline{f}_{AB}}\dfrac{f_{AB}}{k_2^+} + \dfrac{f_{AB}}{k_2^+} - \dfrac{f_A\overline{f}_B + \overline{f}_A f_B - \overline{f}_A\overline{f}_B}{k_2^+\overline{f}_{AB}}}
\end{aligned}
\tag{28}
$$

1   where $f_A = k_A^+ \left[A\right]_T$, $f_B = k_B^+ \left[B\right]_T$, $\overline{f}_A = f_A + k_A^+ \left[E\right]_T$, $\overline{f}_B = f_B + k_B^+ \left[E\right]_T$, $f_{AB} = f_A + f_B$,

2   and $\overline{f}_{AB} = \overline{f}_A + \overline{f}_B$. In equation (28), we assumed $k_2^+ \gg k_A^-$ and $k_2^+ \gg k_B^-$, so that $k_2^+ \approx \tilde{k}_2^+$

3   (we note that this relationship will be used throughout the remainder of this paper). It can

4   then be verified that if $\left[E\right]_T \ll \left[A\right]_T$ and $\left[E\right]_T \ll \left[B\right]_T$, the SUPECA kinetics as

5   represented in equation (28) becomes the SU kinetics in equation (26). Further, if one of

6   the two substrates, say $\left[B\right]_T$, approaches infinity, equation (28) is reduced to

$$\frac{d\left[A\right]_T}{dt} = -\frac{\left[E\right]_T}{\dfrac{1}{k_2^+}\dfrac{\overline{f}_A}{f_A} + \dfrac{1}{f_A}} = -\frac{f_A \left[E\right]_T}{1 + \dfrac{\overline{f}_A}{k_2^+}} \tag{29}$$

7   which by using the definition of f_A and $\overline{f}_A$ can be reduced to the single substrate ECA

8   kinetics equation (Tang, 2015).

9   **3. SUPECA kinetics for a network of reactions**

10   In actual biogeochemical systems, it is more common for many substrates to be

11   processed by many consumers concurrently (and such an assumption is implicitly

12   assumed in the space-time-process unit of any biogeochemical model). To consistently

13   handle such situations, Tang and Riley (2013a) derived the ECA kinetics (see Figure 2

14   for a graphic demonstration) for calculating the consumption of a substrate S_i by a

15   consumer E_j in a network of single substrate reactions $A \xrightarrow{E} products$ as

$$\frac{d[S_i]_{T,j}}{dt} = -\frac{k_{2,ij}^+[E_j]_T\left([S_i]_T/K_{ij}\right)}{1+\sum_{l=1}^{l=I}\left([S_l]_T/K_{lj}\right)+\sum_{l=1}^{l=J}\left([E_l]_T/K_{il}\right)}$$ (30)

1   By defining the normalized substrate flux (with subscript "c" designating that the

2   summation is over a column of the graph in Figure 2)

$$F_{c,j} = \sum_{l=1}^{l=I}\left([S_l]_T/K_{lj}\right) = \sum_{l=1}^{l=I} F_{c,j}^{\{l\}}$$ (31)

3   and its conjugate (with subscript "r" designating that the summation is over a row of the

4   graph in Figure 2)

$$F_{r,i} = \sum_{l=1}^{l=J}\left([E_l]_T/K_{il}\right) = \sum_{l=1}^{l=J} F_{r,i}^{\{l\}}$$ (32)

5   equation (30) can then be rewritten as

$$\frac{d[S_i]_{T,j}}{dt} = -k_{2,ij}^+[E_j]_T\left(\frac{F_{c,j}^{\{i\}}}{1+F_{r,i}+F_{c,j}}\right) = -k_{2,ij}^+[S_i]_T\left(\frac{F_{r,i}^{\{j\}}}{1+F_{r,i}+F_{c,j}}\right)$$ (33)

6   The normalized substrate flux as defined in equation (31) and its conjugate in equation

7   (32) implies that the consumption of substrate S_i by consumer E_j as described by the

8   ECA kinetics in equation (33) may be interpreted as either (i) the potential substrate

9   processing rate of E_j (aka $k_{2,ij}^+[E_j]$) weighted by the relevant importance of the reaction

10   pathway $S_i \xrightarrow{E_j} products$ (aka $F_{c,j}^{\{i\}}$) under the influence of all competing substrate fluxes

1    $F_{c,j}^{\{l\}}$ (towards consumer E_j) and all competing agents' efforts $F_{r,i}^{\{l\}}$ (towards substrate S_i)

2   or (ii) the linear decay potential of S_i (aka $k_{2,ij}^{+}\left[S_i\right]_T$) weighted by relevant importance of

3    $F_{r,i}^{\{j\}}$ under the influence of all competing substrate fluxes and competing agents' efforts.

4   We further note that equations (31) and (32) define some very interesting scaling

5   relationships. For instance, from equation (31), we can define the effective substrate

6   affinity for the bulk substrates ($\left[\bar{S}\right]_T$ defined as the total of all substrates) that are

7   accessible for consumer E_j as

$$K_{E,j} = \left(\sum_{l=1}^{l=l}\left[S_l\right]_T\right)\bigg/F_{c,j} = \left[\bar{S}\right]_T\bigg/F_{c,j} \tag{34}$$

8   Similarly, we can define the effective affinity for substrate S_i resulting from all

9   competing agents as

$$K_{S,i} = \left(\sum_{l=1}^{l=J}\left[E_l\right]_T\right)\bigg/F_{r,i} = \left[\bar{E}\right]_T\bigg/F_{r,i} \tag{35}$$

10   Then by substituting equations (34) and (35) into equation (33), we obtain

$$\begin{aligned}\frac{d\left[S_i\right]_{T,j}}{dt} &= -\frac{k_{2,ij}^{+}\left[E_j\right]_T\left(\left[\bar{S}\right]_T\big/K_{E,j}\right)}{1+\left[\bar{S}\right]_T\big/K_{E,j}+\left[\bar{E}\right]_T\big/K_{S,i}}\frac{F_{c,j}^{\{i\}}}{F_{c,j}} \\ &= -\frac{k_{2,ij}^{+}\left[S_i\right]_T\left(\left[\bar{E}\right]_T\big/K_{S,i}\right)}{1+\left[\bar{S}\right]_T\big/K_{E,j}+\left[\bar{E}\right]_T\big/K_{S,i}}\frac{F_{r,i}^{\{j\}}}{F_{r,i}}\end{aligned} \tag{36}$$

11   which again shows the linear partition in terms of $F_{c,j}^{\{i\}}\big/F_{c,j}$ and $F_{r,i}^{\{j\}}\big/F_{r,i}$.

1   By applying the above two scaling relationships and the three consistent scaling

2   criteria (as we proposed in the introduction section) to the SUPECA kinetics in equation

3   (28), we obtain (in appendix E) the network form of the SUPECA kinetics below,

$$\frac{d[A_i]_{T,jk}}{dt} = -\frac{k_{2,jjk}^{+}[E_k]_T F_{c,A,k}^{\{i\}} F_{c,B,k}^{\{j\}}}{\frac{G_{A,ik}G_{B,jk}}{G_{AB,ijk}}F_{c,AB,k} + F_{c,AB,k} - \frac{F_{c,A,k}G_{B,jk} + G_{A,ik}F_{c,B,k} - G_{A,ik}G_{B,jk}}{G_{AB,ijk}}} \tag{37}$$

4   where

$$F_{c,A,k} = \sum_l F_{c,A,k}^{\{l\}} = \sum_l [A_l]_T \big/ K_{A,lk} \tag{38}$$

$$F_{c,B,k} = \sum_l F_{c,B,k}^{\{l\}} = \sum_l [B_l]_T \big/ K_{B,lk} \tag{39}$$

$$F_{c,AB,k} = F_{c,A,k} + F_{c,B,k} \tag{40}$$

$$F_{r,A,i} = \sum_l [E_l]_T \big/ K_{A,il} \tag{41}$$

$$F_{r,B,j} = \sum_l [E_l]_T \big/ K_{B,jl} \tag{42}$$

$$G_{A,ik} = F_{c,A,k} + F_{r,A,i} \tag{43}$$

$$G_{B,jk} = F_{c,B,k} + F_{r,B,j} \tag{44}$$

$$G_{AB,ijk} = G_{A,ik} + G_{B,jk} \tag{45}$$

1   For equation (37), it is straightforward to verify that if $F_{c,B,k}$ (or $F_{c,A,k}$) goes to infinity,

2   then SUPECA kinetics is reduced to the ECA kinetics in equation (33) . Therefore, the

3   SUPECA kinetics as formulated in equation (37) is an extension of both the SU and ECA

4   kinetics, and SUPECA is applicable for consistent scaling of substrate-consumer

5   networks involving both single-substrate reactions and redox-reactions (a visually more

6   appealing demonstration of the SUPECA kinetics is in Figure 3).

7   **4. Accuracy of the SUPECA kinetics**

8   Following Tang and Riley (2013a), we below evaluate the numerical accuracy of

9   the SUPECA kinetics by comparing its solution against that obtained from solving the

10   equilibrium chemistry problem. However, because of numerical complexity, we restricted

11   the comparison to the AB-E problem as formulated by equations (11)-(16) with the

12   assumption of $k_A^- = k_B^- = 0$ and include a substrate sorbent to mimic a class of

13   biogeochemistry problems in soil, such as aerobic soil ammonium nitrification and

14   aerobic soil organic carbon decomposition (formulated in appendix F).

15   We evaluated the accuracy of SUPECA (equation (37)) and SU (equation (26))

16   over a wide range of parameter values. Specifically, we fixed both substrates at a nominal

17   value of 40 mol m^{-3}, and the maximum substrate processing rate at 48 s^{-1}. Then we

18   sampled the affinity parameters exponentially over the range of $\left[0,1000\right]$ mol m^{-3} and

19   the microbe and sorbent concentrations uniformly over the range of $\left[0,1000\right]$ mol m^{-3}.

20   With a total of 1000 sets of randomly paired parameters, we compared how close the

21   SUPECA and SU approximations are to the EC solution in terms of root mean square

1   error (RMSE) and goodness of linear fit. Because the SU kinetics does not allow a direct

2   integration of the Langmuir adsorption into the calculation of microbe-substrate

3   complexes, we followed Resat et al. (2011) and first solved the Langmuir isotherm to

4   obtain the free substrate concentrations and then entered these free substrate

5   concentrations into SU to obtain the microbe-substrate complex. Apparently, such an

6   artificial ordering in calculation (as needed by the SU approach) suggests that the

7   implementation of SU is numerically cumbersome (and similar numerical difficulties are

8   also associated with the popular MM kinetics (Resat et al., 2011; Tang and Riley,

9   2013a)).

10   Our comparison (Figure 4) clearly indicates that the SUPECA kinetics is superior

11   to the SU kinetics in computing the microbe-substrate complex in presence of the

12   substrate binding competition between microbes and sorbent. The SUPECA kinetics is

13   more accurate in terms of both goodness of linear fitting and RMSE. In magnitude, the

14   RMSE of SUPECA predictions is less than 10% of that of SU calculations. The slope of

15   linear fitting from SUPECA calculations is also much closer to the ideal value 1.0,

16   whereas that from SU calculations is far greater than 1.0, suggesting that SU kinetics

17   significantly overestimates microbe-substrate complexes under a wide range of

18   conditions. This very large slope from SU calculations is also consistent with the

19   singularity at infinite microbial abundances as implied by the linear dependence on

20   microbial abundances in deriving the SU kinetics (equation (26)). Therefore, combined

21   with the better numerical performance of ECA (Tang and Riley, 2013a; Tang, 2015) than

22   MM kinetics, we contend that SUPECA kinetics is both numerically more convenient

23   and more accurate than SU kinetics (which becomes the MM kinetics for one-substrate

1   reactions; see equation (27)) in calculating the microbe-substrate complexes for situations

2   involving microbes, enzymes, substrates and soil minerals (e.g., Tang and Riley, 2015).

3   **5. Example application to modeling aerobic heterotrophic respiration**

4   As an example application, we applied the SUPECA kinetics to model the

5   moisture stress on aerobic soil respiration. In our formulation of the problem (Appendix

6   G), we consider a homogenous 10 cm thick soil with 2.0 mol C m^{-3} microbes and 3.0 mol

7   C m^{-3} dissolvable organic carbon (different DOC values affected our results negligibly as

8   long as they are larger than 0.5 mol C m^{-3}) uniformly distributed across the soil pores. We

9   conceptualize the transport of substrates (i.e., oxygen and DOC) in soil as a two-stage

10   diffusion process (e.g., Grant, 1991) with the first stage from the bulk soil matrix to the

11   water film covering the microbial microsites and the second stage from the water film to

12   the microbial transporters where the substrates are processed. The diffusion processes in

13   soil are calculated based on soil moisture status and the hydraulic properties of a

14   hypothesized soil with a texture of 40% clay and 30% sand. The pedotransfer functions

15   used for calculating soil hydraulic properties are from CLM4.5 (Oleson et al., 2013).

16   Our conceptual model assumes that the inter microsites (or aggregates) transport

17   dominates the intra-aggregate transport, which is consistent with pore scale simulations

18   (Yang et al., 2014). The model is solved to steady state by assuming that the microbes,

19   atmospheric oxygen, and DOC are in balance under the influence of Langmuir type DOC

20   sorption by soil minerals. Calculations are conducted for three levels of soil minerals

21   (with adsorption capacities at 0, 90, and 180 mol C m^{-3}) and two levels of microbial

22   oxygen affinity (with default $K_{O2,w} = 3 \times 10^{-5}$ mol m^{-3} and elevated $K_{O2,w} = 3 \times 10^{-2}$ mol

1   m^{-3}; Figure 5, Figure 6 and Figure 7). The calculation with elevated $K_{O2,w}$ (when

2   compared to the default $K_{O2,w}$) indicates the effect of soil aggregates on determining

3   microbes' moisture response (see explanations below and in Appendix G). We evaluated

4   (1) how close our predicted moisture response function is to the incubation data from

5   Franzluebbers (1999) and (2) how soil mineral adsorption of DOC would affect the shape

6   of the soil moisture response function.

7   When the respiration curves are normalized to the range of $\left[0,1\right]$, we found that

8   all curves have the pattern that soil respiration first increases from dry soil with

9   increasing moisture and then levels off after reaching a peak value (where the respiration

10   is co-limited by oxygen and DOC bioavailability). The curve with the highest mineral

11   soil carbon adsorption capacity (180 mol C m^{-3}) and elevated $K_{O2,w}$ value best

12   approximates the incubation data from Franzluebbers (1999) and as the sorption capacity

13   becomes smaller, the sharper the moisture response function becomes.

14   When the affinity parameter of oxygen is reduced to its default value (while

15   keeping the adsorption capacity to 180 mol C m^{-3}; see explanation in Appendix G), the

16   soil moisture response function becomes the sharpest with the highest threshold moisture

17   where the respiration peaks (see green line in Figure 5). Unlike Kausch and Pallud (2013)

18   and Yang et al. (2014), we here have not explicitly prognosed the oxygen distribution

19   inside the aggregates. Since the apparent oxygen affinity parameter (which we use here)

20   generally increases with aggregate size (Griffin, 1968), the poorer agreement of the data

21   with respect to the prediction using the default oxygen affinity parameter indicates that

22   soil aggregates may play an important role in controlling microbes' response to soil

1   moisture stress. Indeed, Franzluebbers (1999) indicated in his Figure 1 that there are

2   significant amount of aggregates in his incubated soil. Moreover, the higher moisture

3   threshold (where respiration peaks) with the default apparent oxygen affinity parameter is

4   also consistent with measurements that aggregates may facilitate anaerobic processes

5   under well-ventilated conditions (by increasing the range of soil moisture conditions

6   where oxygen limits aerobic processes; Renault and Stengel, 1994).

7   When the effect of different mineral soil carbon adsorption capacity is evaluated

8   against the normalized respiration (Figure 6), we found, being consistent with results

9   described in Tang and Riley (2015), that higher adsorption capacity results in

10   significantly lower soil respiration. Therefore, when the results from Figure 5 and Figure

11   6 are taken together, we contend that, like the soil temperature effect discussed in Tang

12   and Riley (2015), the soil moisture response function is an emergent response resulting

13   from the interactions between biotic and abiotic factors that co-regulate soil organic

14   carbon decomposition (Manzoni et al., 2016). Such a result strongly contrasts with the

15   popular approach in existing soil BGC models (e.g., Koven et al., 2013; Tang et al.,

16   2013), which apply a soil moisture response function as a multiplier on an unstressed

17   rate. We therefore suspect that treating moisture stress as a multiplier in modeling soil C

18   decomposition could also significantly bias existing soil biogeochemical model

19   predictions. We will explore such biases in other studies.

20   When the default oxygen affinity parameter was used in analyzing the effects of

21   different mineral soil carbon adsorption capacities, all the respiration moisture response

22   functions are essentially the same (Figure 7). Since the oxygen affinity parameter reflects

1 the impacts of aggregates at the cm^3 scale, Figures 6 and 7 demonstrate that soil

2 aggregates may have profound influence on soil carbon decomposition rates.

3 **6. Potential applications of the SUPECA kinetics for trait-based biogeochemical**

4 **modeling**

5 Besides the example application above, we expect that the SUPECA kinetics will

6 be a unique and powerful tool for trait-based modeling in various biogeochemical

7 systems. As we show above and below, the SUPECA kinetics will enable more robust

8 predictions with better numerical consistency and smaller parametric sensitivities than the

9 popular family of Monod kinetics, and SUPECA will be applicable for any

10 biogeochemical system that involves substrate-consumer binding and binding

11 competition.

12 The assertion of smaller parametric sensitivity as predicted by SUPECA (than by

13 Monod kinetics) can be verified using the single-substrate reaction network as an

14 example. In this case, SUPECA is reduced to ECA kinetics, and for some substrate S_i in

15 the reaction network, ECA kinetics predicts the sensitivity of its consumption by

16 consumer $\left[E_j \right]$ with respect to the maximum processing rate $k_{2,ij}^+$ as

$$\left| \frac{\partial}{\partial k_{2,ij}^+} \left(\frac{d\left[S_i \right]_{T,j}}{dt} \right) \right| = \frac{\left[E_j \right]_T F_{c,j}^{\{i\}}}{1 + F_{r,i} + F_{c,j}} < \frac{\left[E_j \right]_T F_{c,j}^{\{i\}}}{1 + F_{c,j}} < \frac{\left[E_j \right]_T F_{c,j}^{\{i\}}}{1 + F_{c,j}^{\{i\}}} \tag{46}$$

17 where the term after the first "<" is prediction by the competitive Monod kinetics and that

18 after the second "<" is by the Monod kinetics.

1   To quantitatively evaluate our assertion, we, for instance, apply equation (46) to

2   100 competing substrate fluxes of equal magnitude. We then have $F_{c,j} = 100 F_{c,j}^{\{i\}}$.

3   Meanwhile, if $F_{c,j}^{\{i\}} > 1$, then the sensitivity predicted by competitive Monod kinetics is

4   less than 1% of that by Monod kinetics. Further, if the competing efforts from all agents

5   is comparable to the overall substrate fluxes, i.e., $F_{r,i} \approx F_{c,j}$, then the parametric sensitivity

6   predicted by ECA is about 50% of that by competitive Monod kinetics. Therefore, the

7   ECA (and by extension, SUPECA) prediction is much less sensitive with respect to $k_{2,ij}^{+}$

8   than that predicted by competitive Monod kinetics and Monod kinetics. Moreover, with

9   equations (30) and (37), one can verify that the more substrates and consumers are

10   represented in the system, the smaller the parametric sensitivity will be predicted by the

11   ECA (and SUPECA) kinetics. One can also verify that such robustness is true for other

12   parameters in the SUPECA kinetics, including the substrates and consumer abundances.

13   That including more substrates and consumers will leads to more robust model

14   predictions is the fundamental premise that underlines the proposal of trait-based

15   modeling (e.g., Bouskill et al., 2012), and SUPECA is the only kinetics that explicitly

16   contains this presumption in its formulation.

17   The assertion of wide applicability with SUPECA kinetics has been demonstrated

18   by a number of successful applications that we have published with the ECA kinetics. In

19   a series of studies (Zhu and Riley, 2015; Zhu et al., 2016a, b, c), we show that ECA

20   kinetics was able to significantly improve the modeling of nutrient competition between

21   plants, microbes, and mineral soils. In Tang and Riley (2013a), where the ECA kinetics

22   was first proposed, the lignin decomposition dynamics was correctly captured without *a*

1   *priori* imposing a target lignocellulose index. In Tang and Riley (2013a, 2015) and this

2   study, the ECA kinetics was able to seamlessly incorporate the Langmuir type substrate

3   adsorption into its numerical implementation without invoking the ad hoc numerical

4   order that is prerequisite to MM (or Monod) kinetics for modeling mineral, microbe, and

5   substrate interactions.

6   Finally, we expect the SUPECA kinetics will provide a robust approach to resolve

7   the redox ladder in soil biogeochemistry. Existing approaches have imposed the redox

8   ladder rigorously following some specific order, e.g.

9    $O_2\left(H_2O\right), NO_3^-\left(N_2\right), MnO_2\left(Mn^{2+}\right), Fe\left(OH\right)_3\left(Fe^{2+}\right), SO_4^{2-}\left(H_2S\right), CO_2\left(CH_4\right)$, and

10   $H_2O\left(H_2\right)$ (e.g., Grant, 2001). In contrast, the SUPECA kinetics will allow all these

11   redox-couples to operate concurrently (in any space-time-process unit), a situation that is

12   more consistent with natural soils. Such a feature will also allow the microbial

13   biogeochemistry models (most of which are considered to be valid at pore scale) to be

14   valid at the scale of well-mixed bulk soils ($\sim cm^3$). We are now building such a model and

15   will describe it elsewhere.

16   **7. Conclusion**

17   In this study, we showed that the popular Monod family kinetics and synthesizing

18   unit (SU) kinetics are not scaling consistent for a reaction network involving mixed

19   $A \xrightarrow{E} products$ type and $A+B \xrightarrow{E} products$ type reactions. The SUPECA kinetics, by

20   properly accounting for mass balance constraints of both substrates and consumers, is

21   able to scale such reaction networks without changing its mathematical formulation. Our

Geoscientific
Model Development
Discussions

1   numerical tests indicate that SUPECA kinetics is superior to SU kinetics both in

2   numerical accuracy and numerical robustness and SUPECA kinetics is able to

3   satisfyingly predict the moisture response function of aerobic soil respiration. Moreover,

4   because SUPECA kinetics intrinsically represents specific microbial traits that can be

5   measured, we expect many more novel modeling applications will be plausible to

6   improve predictions of a wide range of biogeochemical systems.

7   **8. Code and data availability**

8   The source code and data used in this manuscript are available upon request to the

9   corresponding author.

10

11   **Appendix A: Deriving the governing equations**

12   The law of mass action formulation of the redox reaction (8) is

$$\frac{d[EA]}{dt} = k_A^+[E][A] + k_B^-[EAB] - \left(k_A^- + k_B^+[B]\right)[EA] \tag{A1}$$

$$\frac{d[EB]}{dt} = k_B^+[E][B] + k_A^-[EAB] - \left(k_B^- + k_A^+[A]\right)[EB] \tag{A2}$$

$$\frac{d[EAB]}{dt} = k_A^+[EB][A] + k_B^+[EA][B] - \left(k_A^- + k_B^- + k_2^+\right)[EAB] \tag{A3}$$

$$\frac{d[P]}{dt} = k_2^+[EAB] \tag{A4}$$

$$\frac{d[A]}{dt} = -k_A^+\left([E] + [EB]\right)[A] + k_A^-\left([EA] + [EAB]\right) \tag{A5}$$

$$\frac{d[B]}{dt} = -k_B^+ \left([E] + [EA] \right)[B] + k_B^- \left([EB] + [EAB] \right) \tag{A6}$$

1   We now apply the total quasi-steady-state approximation (e.g., Borghans et al., 1996) to

2   obtain the Equilibrium Chemistry formulation of the system. Specifically, we obtain

3   equations (11)-(13) by respectively setting the time derivatives of equations (A1)-(A3) to

4   zero. Equation (9) is obtained by adding together equations (A1), (A3) and (A5), and

5   using the definition of $[A]_T$ by equation (14). Equation (10) is obtained by adding

6   together equations (A2), (A3) and (A6) with the definition of $[B]_T$ by equation (15).

7   **Appendix B: Deriving the dual Monod kinetics in equation** (21)**.**

8   Replacing $[EA]$ in equation (17) with that obtained from equation (19), we obtain

$$[EAB] = \frac{[A]}{K_A} \frac{[B]}{K_B} [E] \tag{B-1}$$

9   By solving $[EA]$ from equation (19), $[EB]$ from equation (20) and combining

10   these with equation (B-1) into equation (16), we find

$$[E]_T = \left(1 + \frac{[A]}{K_A} \right)\left(1 + \frac{[B]}{K_B} \right)[E] \tag{B-2}$$

11   Now solve $[E]$ from (B-2) and enter the result into equation (B-1), we then get

$$[EAB] = \left(\frac{[A]}{K_A + [A]} \right)\left(\frac{[B]}{K_A + [B]} \right)[E]_T \tag{B-3}$$

12   We thence obtain the dual Monod kinetics by entering equation (B-3) into

13   equation (9).

14   **Appendix C: Deriving the synthesizing unit kinetics in equation** (26)

1   Since SU kinetics assumes that substrates are not limiting the biogeochemical

2   reaction, we then, from equations (23) and (24), obtain

$$\left[EA\right] = \frac{k_A^+\left[A\right]}{k_B^+\left[B\right]}\left[E\right] \tag{C-1}$$

$$\left[EB\right] = \frac{k_B^+\left[B\right]}{k_A^+\left[A\right]}\left[E\right] \tag{C-2}$$

3   By entering equations (C-1) and (C-2) into equation (13), and solving for $\left[EAB\right]$,

4   we find

$$\left[EAB\right] = \frac{\left[E\right]}{k_2^+ + k_A^- + k_B^-}\left(k_A^+\left[A\right] + k_B^+\left[B\right]\right) = \frac{\left[E\right]}{\tilde{k}_2^+}\left(k_A^+\left[A\right] + k_B^+\left[B\right]\right) \tag{C-3}$$

5   Now if we combine equations (C-1)-(C-3) with equation (16), we get

$$\begin{aligned}
\left[E\right] &= \frac{\left[E\right]_T}{1 + \dfrac{k_A^+\left[A\right]}{k_B^+\left[B\right]} + \dfrac{k_B^+\left[B\right]}{k_A^+\left[A\right]} + \dfrac{k_A^+\left[A\right] + k_B^+\left[B\right]}{\tilde{k}_2^+}} \\[2em]
&= \frac{\left[E\right]_T}{\dfrac{\left(k_A^+\left[A\right] + k_B^+\left[B\right]\right)^2}{\left(k_A^+\left[A\right]\right)\left(k_B^+\left[B\right]\right)} + \dfrac{k_A^+\left[A\right] + k_B^+\left[B\right]}{\tilde{k}_2^+} - 1}
\end{aligned} \tag{C-4}$$

6   which, when combined with equation (C-3), leads to

Geoscientific
Model Development
Discussions

$$
\begin{aligned}
\left[EAB\right] &= \frac{k_A^+\left[A\right]+k_B^+\left[B\right]}{\tilde{k}_2^+} \frac{\left[E\right]_T}{\dfrac{\left(k_A^+\left[A\right]+k_B^+\left[B\right]\right)^2}{\left(k_A^+\left[A\right]\right)\left(k_B^+\left[B\right]\right)}+\dfrac{k_A^+\left[A\right]+k_B^+\left[B\right]}{\tilde{k}_2^+}-1} \\[2em]
&= \frac{\left[E\right]_T\big/\tilde{k}_2^+}{\dfrac{1}{\tilde{k}_2^+}+\dfrac{k_A^+\left[A\right]+k_B^+\left[B\right]}{\left(k_A^+\left[A\right]\right)\left(k_B^+\left[B\right]\right)}-\dfrac{1}{k_A^+\left[A\right]+k_B^+\left[B\right]}} \\[2em]
&= \frac{\left[E\right]_T\big/\tilde{k}_2^+}{\dfrac{1}{\tilde{k}_2^+}+\dfrac{1}{k_A^+\left[A\right]}+\dfrac{1}{k_B^+\left[B\right]}-\dfrac{1}{k_A^+\left[A\right]+k_B^+\left[B\right]}}
\end{aligned}
\tag{C-5}
$$

1   When $\left[EAB\right]$ from equation of (C-5) is entered into equation (9), we then obtain

2   equation (26).

3   **Appendix D: Deriving the SUPECA kinetics equation** (28)

4   We first derive the set of linear equations using the first order closure approach.

5   By entering equations (14)-(16) into equation (23), we have

$$
\begin{aligned}
&k_B^+\left[EA\right]\left(\left[B\right]_T-\left[EB\right]-\left[EAB\right]\right)=k_A^+\left(\left[A\right]_T-\left[EA\right]-\left[EAB\right]\right) \\
&\times\left(\left[E\right]_T-\left[EA\right]-\left[EB\right]-\left[EAB\right]\right)
\end{aligned}
\tag{D-1}
$$

6   Now if we expand equation (D-1), and keep only the zero and the first order term of

7    $\left[EA\right]$, $\left[EB\right]$ and $\left[EAB\right]$, then we obtain

$$
\begin{aligned}
&k_B^+\left[B\right]_T\left[EA\right]=k_A^+\left[E\right]_T\left(\left[A\right]_T-\left[EA\right]-\left[EAB\right]\right) \\
&-k_A^+\left[A\right]_T\left(\left[EA\right]+\left[EB\right]+\left[EAB\right]\right)
\end{aligned}
\tag{D-2}
$$

8   which after some rearrangement becomes

$$
\begin{aligned}
&\left(k_A^+\left[A\right]_T+k_A^+\left[E\right]_T+k_B^+\left[B\right]_T\right)\left[EA\right]+k_A^+\left[A\right]_T\left[EB\right] \\
&+k_A^+\left(\left[A\right]_T+\left[E\right]_T\right)\left[EAB\right]=k_A^+\left[A\right]_T\left[E\right]_T
\end{aligned}
\tag{D-3}
$$

1   Using the definitions of $f_A = k_A^+ [A]_T$, $f_B = k_B^+ [B]_T$ and $\bar{f}_A = f_A + k_A^+ [E]_T$, we may

2   rewrite equation (D-3) as

$$\left(\bar{f}_A + f_B \right)[EA] + f_A [EB] + \bar{f}_A [EAB] = f_A [E]_T \qquad \text{(D-4)}$$

3   Because substrates A and B are symmetric in forming the consumer substrate

4   complexes, a similar linear equation can be derived by switching A and B in equation

5   (D-4) (or by repeating procedures to the derivation of equation (D-4) but using equations

6   (14)-(16) and (24))

$$f_B [EA] + \left(f_A + \bar{f}_B \right)[EB] + \bar{f}_B [EAB] = f_B [E]_T \qquad \text{(D-5)}$$

7   Now substitute equations (14)-(16), (23) and (24) into equation (25) and assume

8   $\tilde{k}_2^+ \approx k_2^+$ (i.e., unbinding is much smaller compared to the product genesis rate), we have

$$\left\{ k_A^+ \left([A]_T - [EA] - [EAB] \right) + k_B^+ \left([B]_T - [EB] - [EAB] \right) \right\}$$
$$\times \left([E]_T - [EA] - [EB] - [EAB] \right) = k_2^+ [EAB] \qquad \text{(D-6)}$$

9   Once again, by dropping the second and higher order terms of the consumer-

10   substrate complexes, equation (D-6) can be reduced to

$$\left(k_A^+ [A]_T + k_B^+ [B]_T \right)[E]_T = \left(k_A^+ [A]_T + k_B^+ [B]_T \right)$$
$$\times \left([EA] + [EB] + [EAB] \right) + k_A^+ [E]_T \left([EA] + [EAB] \right) \qquad \text{(D-7)}$$
$$+ k_B^+ [E]_T \left([EB] + [EAB] \right) + k_2^+ [EAB]$$

11   which by aid of $f_A = k_A^+ [A]_T$, $f_B = k_B^+ [B]_T$, $\bar{f}_A = f_A + k_A^+ [E]_T$, $\bar{f}_B = f_B + k_B^+ [E]_T$,

12   $f_{AB} = f_A + f_B$, and $\bar{f}_{AB} = \bar{f}_A + \bar{f}_B$ becomes

$$\left(\bar{f}_A + f_B \right)[EA] + \left(f_A + \bar{f}_B \right)[EB] + \left(k_2^+ + \bar{f}_{AB} \right)[EAB] = f_{AB} [E]_T \qquad \text{(D-8)}$$

1   Now we solve for $\left[EAB\right]$ from the set of linear equations (D-4), (D-5) and (D-8)

2   using Cramer's rule (e.g., Habgood and Arel, 2012), and find the denominator as

$$\det\left(M_d\right)=\begin{vmatrix} \overline{f}_A+f_B & f_A & \overline{f}_A \\ f_B & f_A+\overline{f}_B & \overline{f}_B \\ \overline{f}_A+f_B & f_A+\overline{f}_B & k_2^+ +\overline{f}_{AB} \end{vmatrix} \tag{D-9}$$

3   and the numerator as

$$\det\left(M_n\right)=\left[E\right]_T\begin{vmatrix} \overline{f}_A+f_B & f_A & f_A \\ f_B & f_A+\overline{f}_B & f_B \\ \overline{f}_A+f_B & f_A+\overline{f}_B & f_{AB} \end{vmatrix} \tag{D-10}$$

4   Equations (D-9) and (D-10) together lead to

$$
\begin{aligned}
\left[EAB\right] &= \frac{\det\left(M_n\right)}{\det\left(M_d\right)} = \frac{f_A f_B \overline{f}_{AB}\left[E\right]_T}{k_2^+\left(f_A\overline{f}_A+f_B\overline{f}_B+\overline{f}_A\overline{f}_B\right)+\overline{f}_A\overline{f}_B f_{AB}} \\
&= \frac{f_A f_B \overline{f}_{AB}\left[E\right]_T}{k_2^+\left(f_{AB}\overline{f}_{AB}-f_A\overline{f}_B-\overline{f}_A f_B+\overline{f}_A\overline{f}_B\right)+\overline{f}_A\overline{f}_B f_{AB}} \\
&= \frac{\left[E\right]_T}{k_2^+\left(\dfrac{f_{AB}}{f_A f_B}-\dfrac{f_A\overline{f}_B+\overline{f}_A f_B-\overline{f}_A\overline{f}_B}{f_A f_B \overline{f}_{AB}}\right)+\dfrac{\overline{f}_A\overline{f}_B f_{AB}}{f_A f_B \overline{f}_{AB}}} \\
&= \frac{\left[E\right]_T / k_2^+}{\dfrac{1}{k_2^+}\dfrac{\overline{f}_A\overline{f}_B f_{AB}}{f_A f_B \overline{f}_{AB}}+\left(\dfrac{1}{f_A}+\dfrac{1}{f_B}-\dfrac{f_A\overline{f}_B+\overline{f}_A f_B-\overline{f}_A\overline{f}_B}{f_A f_B \overline{f}_{AB}}\right)}
\end{aligned}
\tag{D-11}
$$

5   which, when entered into equation (9), leads to equation (28).

6   **Appendix E: Deriving SUPECA for a network of substrates and consumers**

7   In the second equation of equation (33), we show that the consumption of a

8   certain substrate as represented in ECA kinetics is determined by the consumer reaction

1   potential $k_{2,ij}^{+}\left[E_j\right]_T$ multiplied with the relative contribution of the specific consumption

2   pathway with respect to all competing pathways ($F_{c,j}^{\{r\}}\big/\left(1+F_{r,j}+F_{c,j}\right)$). Since SUPECA

3   kinetics is a compatible extension of the ECA kinetics, SUPECA kinetics should have its

4   numerator indicating the potential reaction rate of the specific pathway, and its

5   denominator indicating the efforts of all interacting pathways. Bearing this partition

6   equivalence in mind, therefore, we assert that $\overline{f}_A\big/k_2^{+}$ in equation (29) should be

7   equivalent to $F_{r,i}+F_{c,j}$ in equation (33). This assertion then leads to equations (38), (41)

8   and (43) for A substrates. Similarly, equations (39), (42) and (44) are for B substrates.

9   With the definitions of $f_A\big/k_2^{+}$, $f_B\big/k_2^{+}$, $\overline{f}_A\big/k_2^{+}$ and $\overline{f}_B\big/k_2^{+}$, using the partition

10 equivalence, we can easily define the network form of f_{AB} in equation (40), and the

11 network form of $\overline{f}_{AB}$ in equation (45). Further, we observe that the denominator of the

12 last equation in equation (28) could be rewritten as

13
$$\frac{\left(\overline{f}_A\big/k_2^{+}\right)\left(\overline{f}_B\big/k_2^{+}\right)\left(f_{AB}\big/k_2^{+}\right)}{\left(\overline{f}_{AB}\big/k_2^{+}\right)}+\left(f_{AB}\big/k_2^{+}\right)-\frac{\left(f_A\big/k_2^{+}\right)\left(\overline{f}_B\big/k_2^{+}\right)+\left(\overline{f}_A\big/k_2^{+}\right)\left(f_B\big/k_2^{+}\right)-\left(\overline{f}_A\big/k_2^{+}\right)\left(\overline{f}_B\big/k_2^{+}\right)}{\left(\overline{f}_{AB}\big/k_2^{+}\right)}$$

14 which, after replacing $f_A\big/k_2^{+}$, $f_B\big/k_2^{+}$, $\overline{f}_A\big/k_2^{+}$, $\overline{f}_B\big/k_2^{+}$, $f_{AB}\big/k_2^{+}$ and $\overline{f}_{AB}\big/k_2^{+}$ with their

15 corresponding network forms (i.e. equations (38)-(45)), leads to SUPECA kinetics

16 equation (37).

17 **Appendix F: Formulation of the kinetics-benchmarking problem**

18   Following equations (23)-(25), the Equilibrium Chemistry (EC) problem used to

19 benchmark synthesizing unit (SU) and SUPECA predictions is defined as

$$k_{BS1}\left[B\right]\left[S_1\right]=k_{BS2}\left[S_2\right]\left[BS_1\right] \tag{F-1}$$

$$k_{BS2}\left[B\right]\left[S_2\right]=k_{BS1}\left[S_1\right]\left[BS_2\right] \tag{F-2}$$

$$k_{BS1}\left[BS_2\right]\left[S_1\right]+k_{BS2}\left[BS_1\right]\left[S_2\right]=k_2^+\left[BS_1S_2\right] \tag{F-3}$$

$$K_{MS1}\left[MS_1\right]=\left[M\right]\left[S_1\right] \tag{F-4}$$

1   which are subject to the constraints

$$\left[S_1\right]_T=\left[S_1\right]+\left[MS_1\right]+\left[BS_1\right]+\left[BS_1S_2\right] \tag{F-5}$$

$$\left[S_2\right]_T=\left[S_2\right]+\left[BS_2\right]+\left[BS_1S_2\right] \tag{F-6}$$

$$\left[B\right]_T=\left[B\right]+\left[BS_1\right]+\left[BS_2\right]+\left[BS_1S_2\right] \tag{F-7}$$

$$\left[M\right]_T=\left[M\right]+\left[MS_1\right] \tag{F-8}$$

2   To relate these equations to a dynamic system, S_1 and S_2 are substrates, B is

3   microbial population, and M is some sorbent that can reversibly adsorb substrate S_1.

4   For benchmarking, $\left[BS_1S_2\right]$ is solved from equations (F-1)-(F-8) using a fixed-

5   point iteration algorithm (see supplemental materials) for each set of parameters. Unlike

6   the Newton-Raphson iteration, the fixed-point iteration ensures positive mass of all

7   variables, and mass balance relationships from (F-5)-(F-8) are automatically satisfied by

8   the numerical solution.

9   **Appendix G: Derivation of relevant kinetic parameters for the steady state aerobic**

10   **respiration problem**

11   The aerobic respiration problem is formulated as

$$\frac{d[O_2]_{g,s}}{dt} = \frac{\left([O_2]_a - [O_2]_{g,s}\right)}{(R_a + R_s)Z} - F\left(B, [O_2]_{g,s}, S, M\right) \tag{G-1}$$

1 where $[O_2]_{g,s}$ is gaseous oxygen concentration in bulk soil. $[O_2]_a$ is atmospheric oxygen

2 concentration (set to 8.45 mol m^{-3}). S is dissolvable organic carbon concentration (set to

3 3 mol m^{-3}), and M is soil mineral sorbent concentration (with variable values). All

4 concentrations are defined with unit mol m^{-3}. R_a is aerodynamic resistance, which is set

5 to 50 s m^{-1}. R_s is soil resistance (s m^{-1}) calculated using the approach in Tang and Riley

6 (2013b). Z is soil depth (set to 10 cm). $F\left(B, [O_2]_{g,s}, S, M\right)$ is the oxygen consumption

7 rate calculated using the SUPECA kinetics, whose kinetic parameters are derived as

8 following. The steady-state problem is solved by setting the temporal derivative of

9 equation (G-1) to zero, and solved for $[O_2]_{g,s}$ through iterations. The shape of the flux

10 $F\left(B, [O_2]_{g,s}, S, M\right)$ is then compared to that derived from incubation studies in

11 Franzluebbers (1999).

12   In this aerobic respiration problem, microbes are assumed to form microsites

13 sitting uniformly inside pores of the bulk soil. O_2 approaches the microsites through both

14 aqueous and gaseous diffusion, and only aqueous phase is used for microbial respiration.

15 This leads to the relationship between near cell aqueous O_2 concentration and the

16 diffusive flux as

$$v_m \frac{d[O_2]_{w,0}}{dt} = -k_{O2,w,1}[X][O_2]_{w,0} + \kappa_{O2}\left([O_2]_w - [O_2]_0\right) \tag{G-2}$$

17 where the conductance κ_{O2} is

$$\left(\frac{\kappa_{O2}}{4\pi}\right)^{-1} = \frac{\delta}{D_{w,O2}\, r_m\left(r_m+\delta\right)} + \frac{1}{D_{O2}\left(r_m+\delta\right)} \tag{G-3}$$

1   where r_m is the radius of the microsite (or aggregate), δ is thickness of the water film

2   that covers the microsite (Grant and Rochette, 1994), v_m is the microsite volume (m^3 site$^-$

3   ^{1}), and $\left[O_2\right]$ is the aqueous oxygen concentration in the bulk soil matrix. $\left[X\right]$ is the cell

4   density (mol cell site^{-1}). The unit of $k_{O2,1}$ is then m^3 (mol cell)$^{-1}$ s^{-1}.

5   The bulk aqueous diffusivity in equation (G-3) is

$$D_{O2} = \theta D_{O2,w} + \frac{\varepsilon}{\alpha_{O2}} D_{O2,g} \tag{G-4}$$

6   Now if we assume steady state (aka $d\left[O_2\right]_0 / dt \approx 0$) of equation (G-2), we then

7   obtain

$$\left[O_2\right]_{w,0} = \frac{\left[O_2\right]_w}{1 + \dfrac{k_{O2,w,1}\left[X\right]}{\kappa_{O2}}} \tag{G-5}$$

8   which leads to the revised the affinity parameter as

$$\tilde{K}_{O2} = \frac{k_2}{k_{O2,w,1}}\left(1 + \frac{k_{O2,w,1}\left[X\right]_T}{\kappa_{O2}}\right) \tag{G-6}$$

9   where the zero order approximation is made by taking $\left[X\right] \approx \left[X\right]_T$.

10   Now assume that the ball-like microbe is covered with N disc-like porters, whose

11   mean radius is r_p. Assuming that the binding is limited by diffusion, then using the

12   chemoreception theory by Berg and Purcell (1977), we have

$$k_{O2,w,1} = 4\pi D_{O2,w,0} r_c \frac{Nr_p}{Nr_p + \pi r_c} \text{cell}^{-1} \tag{G-7}$$

1   where the term $Nr_p / (Nr_p + \pi r_c)$ accounts for the interference between different porters of

2   a cell. Thus assuming $[X]_T = m$ cell site^{-1}, we get

$$\tilde{K}_{O2} = \frac{k_2}{k_{O2,w,1}} \left(1 + \frac{k_{O2,1}[X]_T}{\kappa_{O2}} \right) = K_{O2,w} \left(1 + \frac{Nr_p}{Nr_p + \pi r_c} \frac{mr_c}{r_m + \delta} \left(\frac{\delta}{r_m} + \frac{D_{O2,w,0}}{D_{O2}} \right) \right) \tag{G-8}$$

3   With similar procedure, for DOC we have the following

$$\tilde{K}_{DOC} = \frac{k_2}{k_{DOC,w,1}} \left(1 + \frac{k_{DOC,w,1}[X]_T}{\kappa_{DOC}} \right) = K_{DOC} \left(1 + \frac{Nr_p}{Nr_p + \pi r_c} \frac{mr_c}{r_m + \delta} \left(\frac{\delta}{r_m} + \frac{D_{DOC,w,0}}{D_{DOC}} \right) \right) \tag{G-9}$$

4   and

$$k_{DOC,w,1} = 4\pi D_{DOC,w,0} r_c N_A \frac{Nr_p}{Nr_p + \pi r_c} (\text{mol} \cdot \text{cell})^{-1} \tag{G-10}$$

5   where $N_A = 6.02 \times 10^{23} \text{mol}^{-1}$.

6   Below we provide some estimates for the parameters to support the above model

7   of moisture dependence of microbial decomposition. The microbial cell radius r_c is on

8   the order of 10^{-6} m, and r_p / r_c is about 10^{-3}. At 25 °C, the aqueous diffusivity of O_2 is

9   about 2.9×10^{-9} m^2 s^{-1}, therefore, assuming $N = 3000$ porters per cell (which covers only

10   0.3% of the cell's surface area), we have $k_{O2,w,1} = 1.0 \times 10^{10}$ m^3 $(\text{mol cell})^{-1}$ s^{-1}.

11   Similarly, since the aqueous diffusivity of DOC is about 10^{-9} m^2 s^{-1}, assuming $N = 3000$

12   porters per cell, we have $k_{DOC,w,1} = 3.7 \times 10^9$ m^3 $(\text{mol cell})^{-1}$ s^{-1}. Suppose the respiration is

1   bottlenecked by a single respiratory enzyme, and since the enzyme activity varies on the

2   order of 10~1000 s^{-1} (English et al., 2006), then by taking $k_2 = 100N$ s$^{-1} = 3 \times 10^5$ s^{-1} per

3   cell, we have $K_{O2,w} = 3 \times 10^{-5}$ mol m^{-3}, which agrees well with parameters reported for

4   microbes in aqueous solutions in Button (1985). However, Grant (1991) estimated

5    $K_{O2,w} = 3.0 \times 10^{-3}$ mol m^{-3}; Borden and Bedient (1986) estimated

6    $K_{O2,w} = 3.1 \times 10^{-3}$ mol m^{-3} for application in soil. We therefore elevated the numerical

7   value to $K_{O2,w} = 3.0 \times 10^{-3}$ mol m^{-3}. According to equations (G-7) and (G-8), such

8   elevation could occur either by increasing the maximum substrate processing rate k_2 or

9   decreasing the diffusion $k_{O2,w,1}$ controlled parameter (through the formation of micro-

10   pores in aggregates; e.g., Kausch and Pallud, 2013; Yang et al., 2014). Based on similar

11   magnitude analysis, we obtain $K_{DOC,w} = 8.1 \times 10^{-5}$ mol m^{-3}, which falls to the lower end of

12   the values reported for many hydrocarbon compounds as reported in Button (1985). We

13   did not elevate the value of $K_{DOC,w}$ because it could vary over four orders of magnitudes

14   (Button, 1985), and our number leads to a good fit between model predictions and data.

15   Taking all these numbers together, we have

$$\tilde{K}_{O2,w} = K_{O2,w}\left(1 + 0.48 \times \frac{mr_c}{r_m + \delta}\left(\frac{\delta}{r_m} + \frac{D_{O2,w,0}}{D_{O2}}\right)\right)$$
$$= 3 \times 10^{-3}\left(1 + 0.48 \times \frac{mr_c}{r_m + \delta}\left(\frac{\delta}{r_m} + \frac{D_{O2,w,0}}{D_{O2}}\right)\right)$$

(G-11)

$$\tilde{K}_{DOC} = K_{DOC}\left(1 + 0.48 \times \frac{mr_c}{r_m + \delta}\left(\frac{\delta}{r_m} + \frac{D_{DOC,w,0}}{D_{DOC}}\right)\right)$$

$$= 8.1 \times 10^{-5}\left(1 + 0.48 \times \frac{mr_c}{r_m + \delta}\left(\frac{\delta}{r_m} + \frac{D_{DOC,w,0}}{D_{DOC}}\right)\right)$$

(G-12)

1   Since at 25 °C, the Bunsen solubility coefficient of oxygen is 0.032, we have

$$\tilde{K}_{O2,g} = \frac{\tilde{K}_{O2,w}}{0.032} = 9.4 \times 10^{-2}\left(1 + 0.48 \times \frac{mr_c}{r_m + \delta}\left(\frac{\delta}{r_m} + \frac{D_{O2,w,0}}{D_{O2}}\right)\right)$$

(G-13)

2   The water film thickness is a function of soil water potential (Tokunaga, 2009)

3   and we calculate it using the approach in ECOSYS (Grant, 2001), which is

$$\delta = \max\left(10^{-6}, \exp\left(-13.65 - 0.857\log(-\psi)\right)\right)$$

(G-14)

4   where the soil matric potential is of unit m, and water film thickness is restricted to at

5   least 1 μm.

6   For model applications, the microbes are often in the unit of mol C m^{-3}. Bratbak

7   and Dundas (1984) reported that the wet biomass density of bacteria is over the range

8   1.1~1.2 g cm^{-3}, of which about 40% is dry biomass, and about 50% of dry biomass is

9   carbon. Therefore, with the medium cell density 1.15 g cm^{-3}, 1 mol C m^{-3} microbial

10   biomass is about 52.17 cm^3, by further taking $r_c = 10^{-6}$ m=10^{-4} cm, the cell number

11   density is 2.1×10^{-11} mol cell m^{-3}. Therefore, for $k_2 = 100$ s^{-1} per porter, given each cell

12   has 3000 porters, the maximum respiration rate is 6.3×10^{-6} s^{-1} for 1 mol C m^{-3} dry

13   microbial biomass, which was then elevated to 3.8×10^{-4} s^{-1} to obtain a better fitting

14   between data and model prediction. This required elevation in maximum respiration rate

15   indicates that the data as obtained (after 24 days of incubation) in Franzluebbers (1999)

16   are representative of fast growing microbes.

Geoscientific
Model Development
Discussions

1

2

3

4

5 **Author Contributions**

6 J.Y. Tang designed the theory and conducted the analysis. J.Y. Tang and W.J. Riley

7 discussed the results and wrote the paper.

8 **Acknowledgements**

15 **References**

16 Aksnes, D. L. and Egge, J. K.: A theoretical-model for nutrient-uptake in phytoplankton,
17 Mar Ecol Prog Ser, 70, 65-72, 1991.
18 Allison, S. D.: A trait-based approach for modelling microbial litter decomposition, Ecol
19 Lett, 15, 1058-1070, 2012.
20 Armstrong, R. A.: Nutrient uptake rate as a function of cell size and surface transporter
21 density: A Michaelis-like approximation to the model of Pasciak and Gavis, Deep-Sea
22 Res Pt I, 55, 1311-1317, 2008.
23 Arora, V. K., Boer, G. J., Friedlingstein, P., Eby, M., Jones, C. D., Christian, J. R.,
24 Bonan, G., Bopp, L., Brovkin, V., Cadule, P., Hajima, T., Ilyina, T., Lindsay, K.,
25 Tjiputra, J. F., and Wu, T.: Carbon-Concentration and Carbon-Climate Feedbacks in
26 CMIP5 Earth System Models, J Climate, 26, 5289-5314, 2013.

1   Batjes, N. H.: Harmonized soil property values for broad-scale modelling (WISE30sec)

2   with estimates of global soil carbon stocks, Geoderma, 269, 61-68, 2016.

3   Berg, H. C. and Purcell, E. M.: Physics of Chemoreception, Biophys J, 20, 193-219,

4   1977.

5   Blanke, J. H., Lindeskog, M., Lindstrom, J., and Lehsten, V.: Effect of climate data on

6   simulated carbon and nitrogen balances for Europe, J Geophys Res-Biogeo, 121, 1352-

7   1371, 2016.

8   Bonachela, J. A., Raghib, M., and Levin, S. A.: Dynamic model of flexible

9   phytoplankton nutrient uptake, P Natl Acad Sci USA, 108, 20633-20638, 2011.

10 Borden, R. C. and Bedient, P. B.: Transport of dissolved hydrocarbons influenced by

11 oxygen-limited biodegradation .1. Theoretical development, Water Resour Res, 22, 1973-

12 1982, 1986.

13 Borghans, J. A. M., DeBoer, R. J., and Segel, L. A.: Extending the quasi-steady state

14 approximation by changing variables, B Math Biol, 58, 43-63, 1996.

15 Bouskill, N. J., Tang, J.Y., Riley, W. J., and Brodie, E. L.: Trait-based representation of

16 biological nitr fication: model development testing, and predicted community

17 composition, Front Microbiol, 3, 2012.

18 Bouskill, N. J., Riley, W. J., and Tang, J. Y.: Meta-analysis of high-latitude nitrogen-

19 addition and warming studies implies ecological mechanisms overlooked by land models,

20 Biogeosciences, 11, 6969-6983, 2014.

21 Brandt, B. W., van Leeuwen, I. M. M., and Kooijman, S. A. L. M.: A general model for

22 multiple substrate biodegradation. Application to co-metabolism of structurally non-

23 analogous compounds, Water Res, 37, 4843-4854, 2003.Bratbak, G. and Dundas, I.:

24 Bacterial dry-matter content and biomass estimations, Appl Environ Microb, 48, 755-

25 757, 1984.

26 Briggs, G. E. and Haldane, J. B. S.: A note on the kinetics of enzyme action, Biochem J,

27 19, 338-339, 1925.

28 Button, D. K.: Kinetics of nutrient-limited transport and microbial-growth, Microbiol

29 Rev, 49, 270-297, 1985.

30 Chellaboina, V., Bhat, S. P., Haddad, W. M., and Bernstein, D. S.: Modeling and analysis

31 of mass-action kinetics, nonnegativity, realizability, reducibility, and semistability, IEEE

Geoscientific
Model Development
Discussions

1   Contr Syst Mag, 29, 60-78, 2009.

2   Ciais, P., Gasser, T., Paris, J. D., Caldeira, K., Raupach, M. R., Canadell, J. G.,

3   Patwardhan, A., Friedlingstein, P., Piao, S. L., and Gitz, V.: Attributing the increase in

4   atmospheric CO_2 to emitters and absorbers, Nat Clim Change, 3, 926-930, 2013.

5   English, B. P., Min, W., van Oijen, A. M., Lee, K. T., Luo, G. B., Sun, H. Y., Cherayil,

6   B. J., Kou, S. C., and Xie, S. N.: Ever-fluctuating single enzyme molecules: Michaelis-

7   Menten equation revisited (vol 2, pg 87, 2006), Nat Chem Biol, 2, 168-168, 2006.

8   Franzluebbers, A. J.: Microbial activity in response to water-filled pore space of variably

9   eroded southern Piedmont soils, Appl Soil Ecol, 11, 91-101, 1999.

10   Feyman, R.P., Leighton, R.B., and Sands, M.: The Feynman lectures on physics: Vol. I.,

11   Addison-Wesley Publishing Company, Inc., Reading, Massachusetts, 1963

12   Friedlingstein, P., Meinshausen, M., Arora, V. K., Jones, C. D., Anav, A., Liddicoat, S.

13   K., and Knutti, R.: Uncertainties in CMIP5 Climate Projections due to carbon cycle

14   feedbacks, J Climate, 27, 511-526, 2014.

15   Grant, R. F.: A Technique for estimating denitrification rates at different soil

16   temperatures, water Contents, and nitrate concentrations, Soil Sci, 152, 41-52, 1991.

17   Grant, R. F. and Rochette, P.: Soil microbial respiration at different water potentials and

18   temperatures - theory and mathematical-modeling, Soil Sci Soc Am J, 58, 1681-1690,

19   1994.

20   Grant, R.F.: A review of the canadian ecosystem Model-Ecosys, in Modeling carbon and

21   nitrogen dynamics for soil management, 173-264, 2001.

22   Griffin, D. M.: A Theoretical study relating concentration and diffusion of oxygen to

23   biology of organisms in soil, New Phytol, 67, 561-577, 1968.

24   Gross, D., Shortle, J.F., Thompson, J.M. and Harris, C.M.: Fundamentals of queueing

25   theory, ISBN: 978-1-118-21164-9, Wiley series in probability and statistics, 2011.

26   He, Y. J., Trumbore, S. E., Torn, M. S., Harden, J. W., Vaughn, L. J. S., Allison, S. D.,
27   and Randerson, J. T.: Radiocarbon constraints imply reduced carbon uptake by soils
28   during the 21st century, Science, 353, 1419-1424, 2016.
29   Holling, C. S.: Some characteristics of simple types of predation and parasitism, Can.

30   Entomol., 91, 385–398, doi:10.4039/Ent91385-7, 1959.

31   Holling, C.S.: The functional response of invertebrate predators to prey density, Mem.

32   Entomol. Soc. Can., 48, 1-86, 1966.

Geoscientific
Model Development
Discussions

1   Kausch, M. F. and Pallud, C. E.: Modeling the impact of soil aggregate size on selenium

2   immobilization, Biogeosciences, 10, 1323-1336, 2013.

3   Kolditz, O., Ratke, R., Diersch, H. J. G., and Zielke, W.: Coupled groundwater flow and

4   transport .1. Verification of variable density flow and transport models, Adv Water

5   Resour, 21, 27-46, 1998.

6   Kooijman, S. A. L. M.: The Synthesizing Unit as model for the stoichiometric fusion and

7   branching of metabolic fluxes, Biophys Chem, 73, 179-188, 1998.

8   Kooijman, S.: Dynamic energy budget theory for metabolic organisation. Cambridge

9   University Press, Cambridge, 2010.

10 Koven, C. D., Riley, W. J., Subin, Z. M., Tang, J. Y., Torn, M. S., Collins, W. D., Bonan,

11 G. B., Lawrence, D. M., and Swenson, S. C.: The effect of vertically resolved soil

12 biogeochemistry and alternate soil C and N models on C dynamics of CLM4,

13 Biogeosciences, 10, 7109-7131, 2013.

14 Le Roux, X., Bouskill, N. J., Niboyet, A., Barthes, L., Dijkstra, P., Field, C. B., Hungate,

15 B. A., Lerondelle, C., Pommier, T., Tang, J. Y., Terada, A., Tourna, M., and Poly, F.:

16 Predicting the responses of soil nitrite-oxidizers to multi-factorial global change: A trait-

17 based approach, Front Microbiol, 7, 2016.

18 Litchman, E. and Klausmeier, C. A.: Trait-based community ecology of phytoplankton,

19 Annu Rev Ecol Evol S, 39, 615-639, 2008.

20 Luo, Z., Wang, E., Zheng, H., Baldock, J. A., Sun, O. J., and Shao, Q.: Convergent

21 modelling of past soil organic carbon stocks but divergent projections, Biogeosciences,

22 12, 4373-4383, 2015.

23 Manzoni, S., Moyano, F., Katterer, T., and Schimel, J.: Modeling coupled enzymatic and

24 solute transport controls on decomposition in drying soils, Soil Biol Biochem, 95, 275-

25 287, 2016.

26 Mao, X., Prommer, H., Barry, D. A., Langevin, C. D., Panteleit, B., and Li, L.: Three-

27 dimensional model for multi-component reactive transport with variable density

28 groundwater flow, Environ Modell Softw, 21, 615-628, 2006.

29 Michaelis, L. and Menten, M. L.: The kenetics of the inversion effect,

30 Biochem. Z., 49, 333–369, 1913.

31 Monod, J.: The growth of bacterial cultures, Annu Rev Microbiol, 3, 371-394, 1949.

1   Murdoch, W. W.: Functional response of predators, J Appl Ecol, 10, 335-342, 1973.

2   Oleson, K.W. et al.: Technical description of version 4.5 of the Community Land Model

3   (CLM). Ncar TechRep., Note NCAR/TN-503+ STR. National Center for Atmospheric

4   Research, Boulder, CO, 422 pp. doi: 10.5065/D6RR1W7M, 2013

5   Pyun, C. W.: Steady-state and equilibrium approximations in chemical kinetics, J Chem

6   Educ, 48, 194-&, 1971.

7   Renault, P. and Stengel, P.: Modeling oxygen diffusion in aggregated Soils .1.

8   Anaerobiosis inside the aggregates, Soil Sci Soc Am J, 58, 1017-1023, 1994.

9   Resat, H., Bailey, V., McCue, L.A., and Konopka, A.: Modeling microbial dynamics in

10 heterogeneous environments: growth on soil carbon sources, Microb. Ecol.,

11 doi:10.1007/s00248-011-9965-x, 2011.

12 Reuveni, S., Urbakh, M., and Klafter, J.: Role of substrate unbinding in Michaelis-

13 Menten enzymatic reactions, P Natl Acad Sci USA, 111, 4391-4396, 2014.

14 Riley, W. J., Subin, Z. M., Lawrence, D. M., Swenson, S. C., Torn, M. S., Meng, L.,

15 Mahowald, N. M., and Hess, P.: Barriers to predicting changes in global terrestrial

16 methane fluxes: analyses using CLM4Me, a methane biogeochemistry model integrated

17 in CESM, Biogeosciences, 8, 1925-1953, 2011.

18 Riley, W. J., Maggi, F., Kleber, M., Torn, M. S., Tang, J. Y., Dwivedi, D., and Guerry,

19 N.: Long residence times of rapidly decomposable soil organic matter: application of a

20 multi-phase, multi-component, and vertically resolved model (BAMS1) to soil carbon

21 dynamics, Geosci Model Dev, 7, 1335-1355, 2014.

22 Shao, P., Zeng, X. B., Sakaguchi, K., Monson, R. K., and Zeng, X. D.: Terrestrial carbon

23 cycle: climate relations in eight CMIP5 earth system models, J Climate, 26, 8744-8764,

24 2013.

25 Shi, M., Fisher, J. B., Brzostek, E. R., and Phillips, R. P.: Carbon cost of plant nitrogen

26 acquisition: global carbon cycle impact from an improved plant nitrogen cycle in the

27 Community Land Model, Global Change Biol, 22, 1299-1314, 2016.

28 Sulman, B. N., Phillips, R. P., Oishi, A. C., Shevliakova, E., and Pacala, S. W.: Microbe-

29 driven turnover offsets mineral-mediated storage of soil carbon under elevated CO2, Nat

30 Clim Change, 4, 1099-1102, 2014.

31 Tang, J. Y. and Zhuang, Q. L.: Equifinality in parameterization of process-based

1 biogeochemistry models: A significant uncertainty source to the estimation of regional

2 carbon dynamics, J Geophys Res-Biogeo, 113, 2008.

3 Tang, J. Y. and Zhuang, Q. L.: A global sensitivity analysis and Bayesian inference

4 framework for improving the parameter estimation and prediction of a process-based

5 Terrestrial Ecosystem Model, J Geophys Res-Atmos, 114, 2009.

6 Tang, J.Y., Zhuang, Q., Shannon, R. D., and White, J. R.: Quantifying wetland methane

7 emissions with process-based models of different complexities, Biogeosciences, 7, 3817-

8 3837, 2010.

9 Tang, J. Y. and Riley, W. J.: A total quasi-steady-state formulation of substrate uptake

10 kinetics in complex networks and an example application to microbial litter

11 decomposition, Biogeosciences, 10, 8329-8351, 2013a.

12 Tang, J. Y. and Riley, W. J.: A new top boundary condition for modeling surface

13 diffusive exchange of a generic volatile tracer: theoretical analysis and application to soil

14 evaporation, Hydrol Earth Syst Sc, 17, 873-893, 2013b.

15 Tang, J. Y., Riley, W. J., Koven, C. D., and Subin, Z. M.: CLM4-BeTR, a generic

16 biogeochemical transport and reaction module for CLM4: model development,

17 evaluation, and application, Geosci Model Dev, 6, 127-140, 2013.

18 Tang, J. Y. and Riley, W. J.: Weaker soil carbon-climate feedbacks resulting from

19 microbial and abiotic interactions, Nat Clim Change, 5, 56-60, 2015.

20 Tang, J. Y.: On the relationships between the Michaelis-Menten kinetics, reverse

21 Michaelis-Menten kinetics, equilibrium chemistry approximation kinetics, and quadratic

22 kinetics, Geosci Model Dev, 8, 3823-3835, 2015.

23 Tang, J. Y. and Riley, W. J.: Technical Note: A generic law-of-the-minimum flux limiter

24 for simulating substrate limitation in biogeochemical models, Biogeosciences, 13, 723-

25 735, 2016.

26 Todd-Brown, K. E. O., Randerson, J. T., Post, W. M., Hoffman, F. M., Tarnocai, C.,

27 Schuur, E. A. G., and Allison, S. D.: Causes of variation in soil carbon simulations from

28 CMIP5 Earth system models and comparison with observations, Biogeosciences, 10,

29 1717-1736, 2013.

30 Tokunaga, T. K.: Hydraulic properties of adsorbed water films in unsaturated porous

31 media, Water Resour Res, 45, 2009.
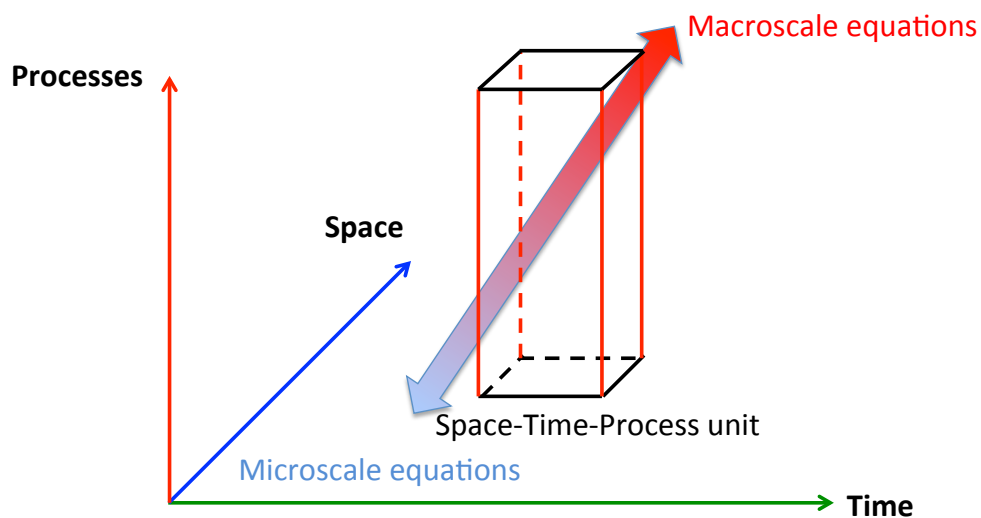
Geoscientific
Model Development
Discussions

1 Van Slyke, D. D. and Cullen, G. E.: The mode of action of urease and of enzymes in

2 general, J Biol Chem, 19, 141-180, 1914.

3 Vitousek, P.: Nutrient cycling and nutrient use efficiency, Am Nat, 119, 553-572, 1982.

4 Wang, Y. P., Leuning, R., Cleugh, H. A., and Coppin, P. A.: Parameter estimation in

5 surface exchange models using nonlinear inversion: how many parameters can we

6 estimate and which measurements are most useful?, Global Change Biol, 7, 495-510,

7 2001.

8 Wieder, W. R., Bonan, G. B., and Allison, S. D.: Global soil carbon projections are

9 improved by modelling microbial processes, Nat Clim Change, 3, 909-912, 2013.

10 Wieder, W. R., Grandy, A. S., Kallenbach, C. M., and Bonan, G. B.: Integrating

11 microbial physiology and physio-chemical principles in soils with the MIcrobial-MIneral

12 Carbon Stabilization (MIMICS) model, Biogeosciences, 11, 3899-3917, 2014.

13 Wieder, W. R., Cleveland, C. C., Lawrence, D. M., and Bonan, G. B.: Effects of model

14 structural uncertainty on carbon cycle projections: biological nitrogen fixation as a case

15 study, Environ Res Lett, 10, 2015a.

16 Wieder, W. R., Allison, S. D., Davidson, E. A., Georgiou, K., Hararuk, O., He, Y. J.,

17 Hopkins, F., Luo, Y. Q., Smith, M. J., Sulman, B., Todd-Brown, K., Wang, Y. P., Xia, J.

18 Y., and Xu, X. F.: Explicitly representing soil microbial processes in Earth system

19 models, Global Biogeochem Cy, 29, 1782-1800, 2015b.

20 Wieder, W. R., Cleveland, C. C., Smith, W. K., and Todd-Brown, K.: Future productivity

21 and carbon storage limited by terrestrial nutrient availability, Nat Geosci, 8, 441-444,

22 2015c.

23 Williams, P. J.: Validity of application of simple kinetic analysis to heterogeneous

24 microbial populations, Limnol Oceanogr, 18, 159-164, 1973.

25 Williams, M., Schwarz, P. A., Law, B. E., Irvine, J., and Kurpius, M. R.: An improved

26 analysis of forest carbon dynamics using data assimilation, Global Change Biol, 11, 89-

27 105, 2005.

28 Yang, X. F., Richmond, M. C., Scheibe, T. D., Perkins, W. A., and Resat, H.: Flow

29 partitioning in fully saturated soil aggregates, Transport Porous Med, 103, 295-314, 2014.

30 Yeh, G. T., Burgos, W. D., and Zachara, J. M.: Modeling and measuring biogeochemical

31 reactions: system consistency, data needs, and rate formulations, Adv Environ Res, 5,

1   219-237, 2001.

2   Zhu, Q. and Riley, W. J.: Improved modelling of soil nitrogen losses, Nat Clim Change,

3   5, 705-706, 2015.

4   Zhu, Q., Riley, W. J., Tang, J.Y., and Koven, C. D.: Multiple soil nutrient competition

5   between plants, microbes, and mineral surfaces: model development, parameterization,

6   and example applications in several tropical forests, Biogeosciences, 13, 341-363, 2016a.

7   Zhu, Q., Riley, W. J. and Tang, J.Y.: A new theory of plant-microbe nutrient competition

8   resolves inconsistencies between observations and model predictions. Ecol Appl.

9   Accepted Author Manuscript. doi:10.1002/eap.1490, 2016b

10 Zhu, Q., Iversen, C. M., Riley, W. J., Slette, I. J., and Vander Stel, H. M.: Root traits

11 explain observed tundra vegetation nitrogen uptake patterns: Implications for trait-based

12 land models, J. Geophys. Res. Biogeosci., 121, 3101–3112, doi:10.1002/2016JG003554,
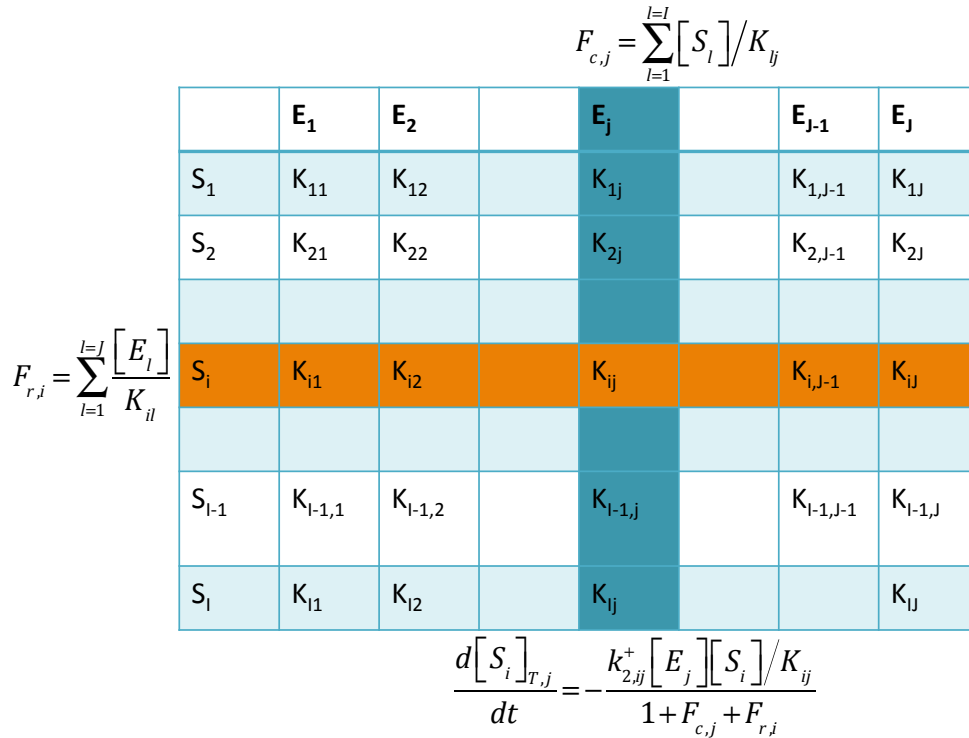
13 2016c.

14

15

16

17

The scaling dimensions for numerical modeling of physical systems

Figure 1. Relationships of the three dimensions involved in the scaling exercise for numerical modeling of biogeochemical systems. In general, as one scales the Space-Time-Process unit from small scales into large scales, the resultant macroscale equations may appear simpler than the microscale equations.
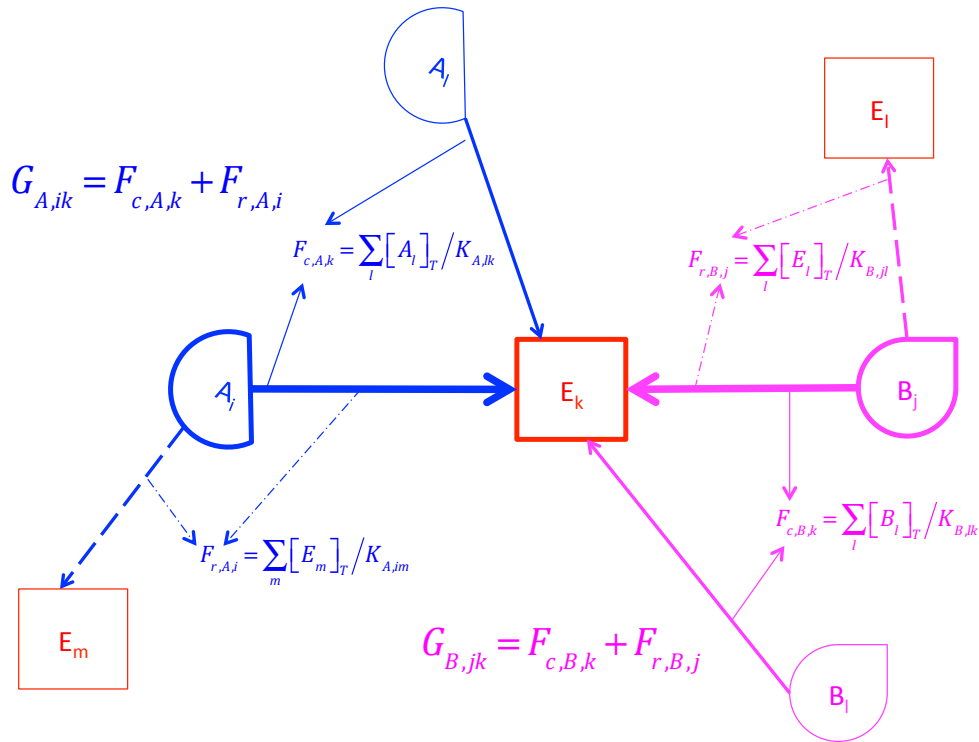
$$F_{c,j} = \sum_{l=1}^{l=I} \big[S_l \big] \big/ K_{lj}$$

	E_1	E_2		E_j		E_{J-1}	E_J
S_1	K_{11}	K_{12}		K_{1j}		$K_{1,J-1}$	K_{1J}
S_2	K_{21}	K_{22}		K_{2j}		$K_{2,J-1}$	K_{2J}
S_i	K_{i1}	K_{i2}		K_{ij}		$K_{i,J-1}$	K_{iJ}
S_{I-1}	$K_{I-1,1}$	$K_{I-1,2}$		$K_{I-1,j}$		$K_{I-1,J-1}$	$K_{I-1,J}$
S_I	K_{I1}	K_{I2}		K_{Ij}			K_{IJ}

$$F_{r,i} = \sum_{l=1}^{l=J} \frac{\big[E_l \big]}{K_{il}}$$

$$\frac{d\big[S_i \big]_{T,j}}{dt} = - \frac{k_{2,ij}^{+} \big[E_j \big] \big[S_i \big] \big/ K_{ij}}{1 + F_{c,j} + F_{r,i}}$$

1

2 Figure 2. Graph representation of the ECA kinetics as derived in Tang and Riley (2013a).

3 The equation in blue shows the uptake of substrate S_i by consumer E_j as a function the

4 normalized substrate flux $F_{c,j}$ and its conjugate flux $F_{r,i}$. Here subscript "c" designates

5 column, and "r" designates row.

6
7
8
9

An example unit block for applying the network-oriented SUPECA kinetics

1

Figure 3. Graph representation for the relationships between substrates, consumers, and normalized fluxes and their conjugates for a block unit of a large substrate-consumer network.
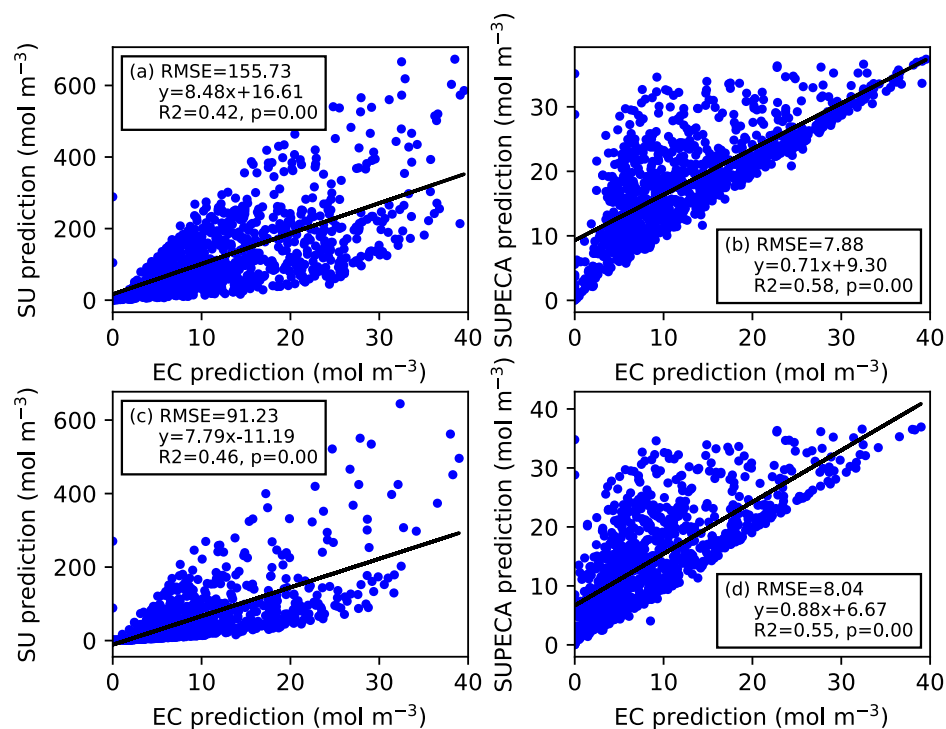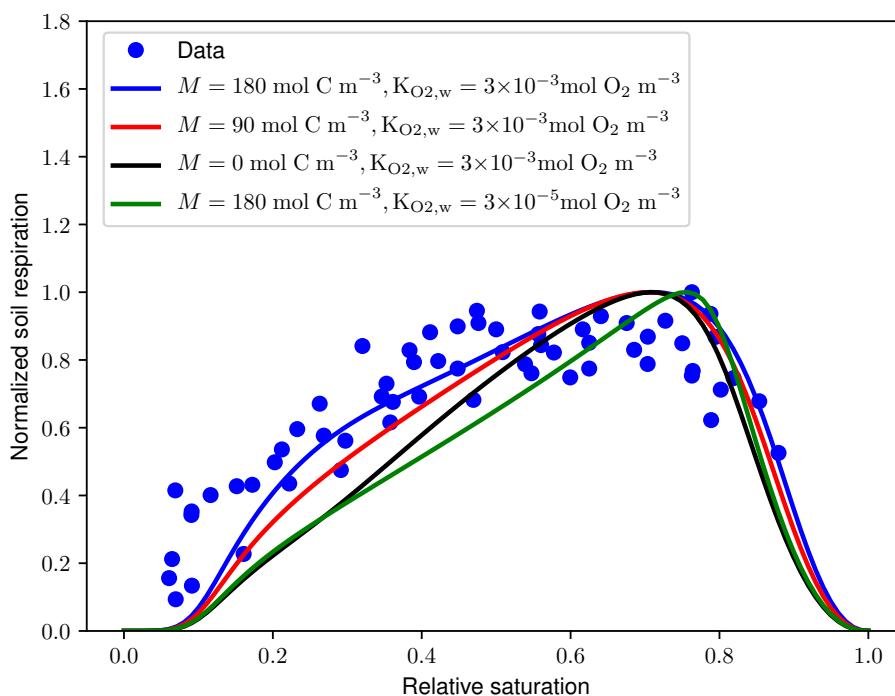
5
6
7
8
9
10
11
12
13
14
15
16
17
18
19
20

1
2　Figure 4. Benchmark of the SU (left column) and SUPECA (right column) predictions
3　against those by the full EC formulation. We note that the y-axes of the left panels are of
4　much larger scale than those on the right. The problem is formulated in Appendix F.
5　Panels (a) and (b) are for the case when $M = 0$; panels (c) and (d) are for uniformly
6　distributed $M > 0$. The related distributions of parameters are in Figure S1 of the
7　supplemental material.

8
9
10
11
12
13
14
15
16
17
18
19
20
21
22
23
24

1

2
3   Figure 5. Comparison of predicted normalized soil moisture response functions to that
4   derived from incubation data from Franzluebbers (1999). All response functions are
5   normalized with their respective peak respiration.

6
7
8
9
10
11
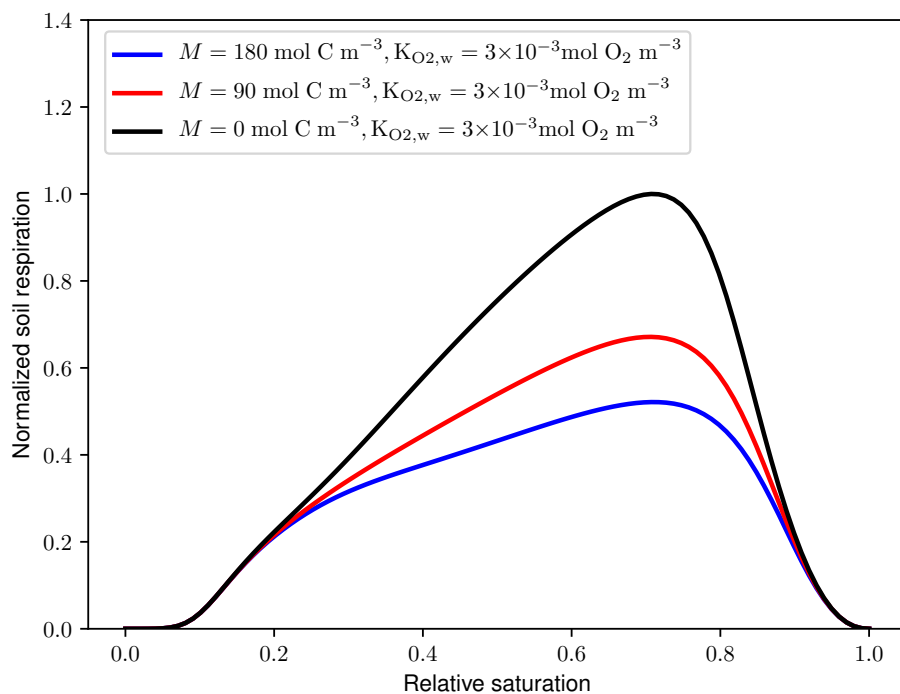12
13
14
15
16
17
18
19
20
21
22
23
24
25

1

2
3 Figure 6. Simulated moisture response functions using elevated affinity parameter for O_2.
4 The respiration data are normalized with the peak value from the case with zero soil
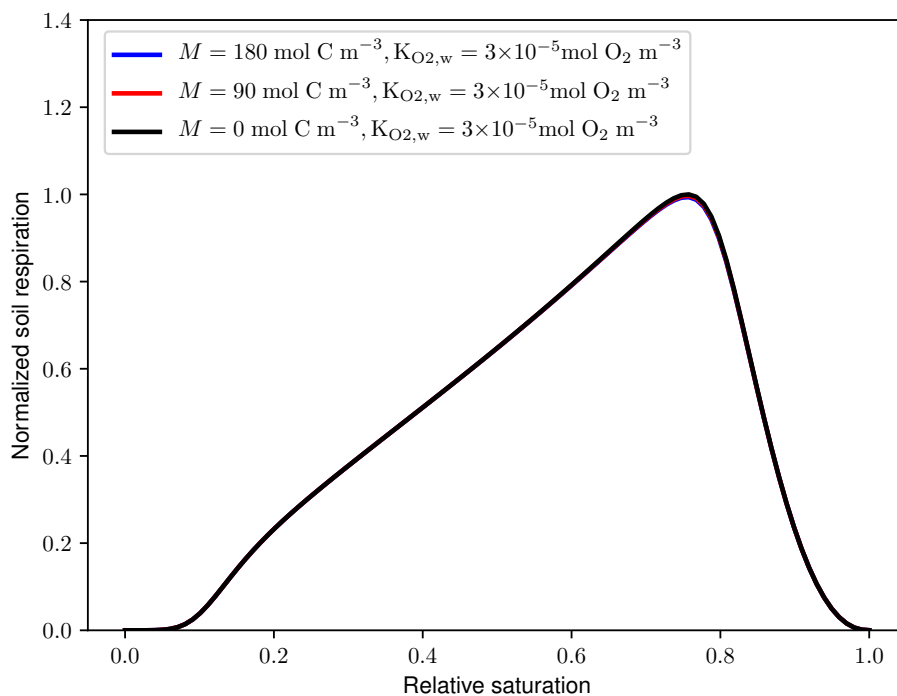5 minerals (i.e., black line in Figure).

6

7
8
9
10
11

1
2   Figure 7. Simulated moisture response functions using default affinity parameter for O_2.
3   The respiration data are normalized with the peak value from the case with zero soil
4   minerals (i.e., black line in Figure). Note here all three lines overlap each other almost
5   perfectly.